

Dynamics of HIV Infection of CD4⁺ T cells

ALAN S. PERELSON

Theoretical Division, Los Alamos National Laboratory, Los Alamos, New Mexico

DENISE E. KIRSCHNER

Department of Mathematics, Vanderbilt University, Nashville, Tennessee

AND

ROB DE BOER*

Theoretical Division, Los Alamos National Laboratory, Los Alamos, New Mexico

Received 22 January 1992; revised 21 July 1992

ABSTRACT

We examine a model for the interaction of HIV with CD4⁺ T cells that considers four populations: uninfected T cells, latently infected T cells, actively infected T cells, and free virus. Using this model we show that many of the puzzling quantitative features of HIV infection can be explained simply. We also consider effects of AZT on viral growth and T-cell population dynamics.

The model exhibits two steady states, an uninfected state in which no virus is present and an endemically infected state, in which virus and infected T cells are present. We show that if N , the number of infectious virions produced per actively infected T cell, is less a critical value, N_{crit} , then the uninfected state is the only steady state in the nonnegative orthant, and this state is stable. For $N > N_{\text{crit}}$, the uninfected state is unstable, and the endemically infected state can be either stable, or unstable and surrounded by a stable limit cycle. Using numerical bifurcation techniques we map out the parameter regimes of these various behaviors. Oscillatory behavior seems to lie outside the region of biologically realistic parameter values. When the endemically infected state is stable, it is characterized by a reduced number of T cells compared with the uninfected state. Thus T-cell depletion occurs through the establishment of a new steady state. The dynamics of the establishment of this new steady state are examined both numerically and via the quasi-steady-state approximation. We develop approximations for the dynamics at early times in which the free virus rapidly binds to T cells, during an intermediate time scale in which the virus grows exponentially, and a third time scale on which viral growth slows and the endemically infected steady state is approached. Using the quasi-steady-state approx-

*Present address: Bioinformatics Group, University of Utrecht, Padualaan 8, 3584 CH Utrecht, The Netherlands.

imation the model can be simplified to two ordinary differential equations the summarize much of the dynamical behavior. We compute the level of T cells in the endemically infected state and show how that level varies with the parameters in the model. The model predicts that different viral strains, characterized by generating differing numbers of infective virions within infected T cells, can cause different amounts of T-cell depletion and generate depletion at different rates.

Two versions of the model are studied. In one the source of T cells from precursors is constant, whereas in the other the source of T cells decreases with viral load, mimicking the infection and killing of T-cell precursors. The latter gives more realistic predictions than the model with a constant source.

1. INTRODUCTION

One of the consequences of infection by the human immunodeficiency virus (HIV) is the selective depletion of $CD4^+$ T cells, the cells commonly known as helper T cells or T4 cells. Because of the central role of $CD4^+$ T cells in immune regulation, their depletion can have widespread deleterious effects on the functioning of the immune system as a whole. In fact, the decline in the number of $CD4^+$ T cells in peripheral blood and the peripheral blood ratio of $CD4^+/CD8^+$ T cells are both used in a clinical setting as indicators of the disease stage [20, 50, 53, 58]. In this paper we present and analyze a simple model for the population dynamics of $CD4^+$ T cells in the presence and absence of HIV. We feel it is important that any model that purports to quantitatively characterize the effects of HIV infection be able to make realistic predictions about the status of the immune system in the absence of HIV infection. To focus the model on the effects of HIV on T-cell population dynamics, we do not deal with the dynamics of the immune response to HIV. Such a response is generally present, and one could assume that there is a constant level of immune defense that influences parameters in the model. Here we are interested in the question of whether HIV infection by itself can account for T-cell depletion in seropositive patients, and hence we not pursue the potential effects of immune defenses.

Over the past decade, a number of models have been developed to describe the immune system and its interaction with HIV. Both stochastic and deterministic models have been developed. Stochastic models, such as the ones presented by Merrill [42, 43], can be used to account for the early events in the disease when there are few infected cells and a small number of viruses, or in situations where the variability among individuals is of interest. The model of Nowak and coworkers [47, 48] looks at the effects of variability among viral strains. Deterministic models, such as the ones developed by Cooper [7], Intrator et al. [30], McLean [38], McLean and Kirkwood [39], Reibnegger et al. [54], Doležal

and Hraba [10, 28], Hraba et al. [29], Fletcher et al. [16], Anderson and May [4], and Perelson [49], examine the changes in mean cell numbers and are more applicable to later stages of the process in which population sizes are large. These models typically consider the dynamics of the CD4⁺ helper and virus populations. In some of these models, other immune system populations such as B cells or CD8⁺ cells have been included.

The model explored here is aimed at explaining a number of quantitative features of HIV infection that are unusual and, in the absence of a model, perplexing. As we shall show, our basic model can account for the long latency between infection and the onset of clinical AIDS as well as the low concentration of free virus observed in the blood. The model exhibits substantial CD4⁺ T-cell depletion but in its current form is unable to obtain the very low CD4⁺ cell counts seen during the late stages of the disease, particularly if the frequency of latently infected CD4⁺ T cells is kept at realistically low levels and the long latency period is maintained. The depletion of CD4⁺ cells has been particularly puzzling, since only 1 in 10⁴–10⁵ cells in the peripheral blood of infected HIV individuals expresses viral proteins or mRNA [14, 24] and only 1 in 10²–10³ T cells harbors viral DNA [55, 56]. In view of the natural turnover of CD4⁺ T cells in the body, it would seem that the T-cell pool should be able to compensate for such a low rate of T-cell infection [14]. Our work partially supports this observation, in that extreme reduction of CD4⁺ cells occurs only in the version, of our model with a constant source of T cells if the population of latently infected cells is larger than that observed. Realistic population levels of latently and actively infected cells, as well as long latency and low blood viremia, are obtained in a second version of the model in which T-cell precursors can be infected, thus reducing the supply of new T cells to the periphery. Thus the natural turnover and replenishment of T cells may be important processes in determining the CD4⁺ T cell count in AIDS patients.

The model developed here is not meant to be a comprehensive model of HIV's interaction with the immune system. It is aimed at examining the kinetics and degree of T-cell depletion that can be caused by viral cytopathicity and thus does not deal with the immune response to HIV. However, there have been a number of observations of viral strains that appear not to induce an effective immune response; these strains have been called escape mutants. Such strains are observed to be of the slow/low type [2]; that is, they replicate slowly and have low expression in CD4⁺ T cells. Generally, virus isolated during the latent period is of the slow/low type, while rapid/high strains are characteristically isolated during the period of active AIDS. Rapid/high

strains have also been isolated during a period of initial HIV viremia, which often follows infection [60]. It has been suggested that the anti-HIV immune response that seems to occur during or following the initial viremia is able to suppress rapid/high strains, whereas the slow/low strains are able to avoid the immune response.

Nelson and Perelson [46] presented a model that shows how some viral variants may be able to escape generating an effective immune response. In that model, consistent with observations, the escape mutants are of the slow/low type. The model presented in this paper deals with viral strains that, though not identical in their activity to the escape mutants considered in [46], still have the property of slow replication in $CD4^+$ T cells. Thus, our model, which ignores an immune response, may in fact be relevant to the population dynamics of slow/low escape mutants. We also use our model to show that if slow/low strains are replaced by rapid/high strains in end-stage disease, then significant T-cell depletion, approaching that seen in patients, can be obtained in the model.

2. MODEL

To generate a realistic model of T-cell infection by HIV, we first need to consider the population dynamics of T cells in the absence of HIV. T cells, like other lymphocytes, are produced in the bone marrow. Immature cells migrate to the thymus, where they undergo further differentiation and maturation into immunocompetent T cells. The thymus is subject to involution, a decrease in weight and volume associated with microscopic evidence of degeneration. In humans, the thymus reaches its greatest weight at about the time of puberty and then begins to gradually involute [61]. Removal of the thymus from an adult usually has minimal effects, although the adult thymus is functional and some of its lymphocytes serve as T-cell precursors and immunocompetent T cells [12]. Within healthy individuals the number of T cells in the blood is maintained relatively constant, with $CD4^+$ T cells comprising about 1000 cells/mm³ [34]. The model discussed here focuses on $CD4^+$ T cells. Thus we shall use the term T cell to mean $CD4^+$ T cell throughout the remainder of this paper.

2.1. T-CELL GROWTH IN AN UNINFECTED INDIVIDUAL

As a model of T-cell dynamics we propose

$$\frac{dT}{dt} = s + rT \left(1 - \frac{T}{T_{\max}} \right) - \mu_T T, \quad (1)$$

where T is the number of CD4⁺ T cells, as measured in the blood, say. The three terms in the equation represent the rates of production and destruction of T cells, s being the rate of supply of immunocompetent T cells from precursors in the thymus. T cells, like all cells in the body, have a finite lifetime. The lifetime may vary among T cells, with memory T cells thought to have a longer life span than virgin T cells. Here we do not distinguish between these classes of T cells, and thus μ_T in Equation (1) represents the average per capita death rate of T cells. T cells, when stimulated by antigen or mitogen, can divide and increase in population. We assume that the growth of T cells is governed by a logistic equation, where r is the average specific T-cell growth rate obtained in the absence of population limitation. As will be discussed in more detail in the next section, r depends on the average degree of antigen or idiotypic network stimulation of T-cell proliferation. However, even when highly stimulated, the total number of T cells in the body remains bounded. The term in parentheses shuts off T-cell growth as the population level T_{\max} is approached from below.

Let T_0 denote the normal steady-state T-cell population size found by solving

$$f(T) = s + rT \left(1 - \frac{T}{T_{\max}} \right) - \mu_T T = 0, \quad (2)$$

that is,

$$T_0 = \frac{T_{\max}}{2r} \left\{ r - \mu_T + \left[(r - \mu_T)^2 + \frac{4sr}{T_{\max}} \right]^{1/2} \right\}. \quad (3)$$

The other root of Equation (2) is negative, and thus Equation (3) represents the only physically possible steady state of the system.

There are certain parameter restrictions that we shall impose to ensure that this model gives realistic population dynamics. Even after thymic involution, the thymus remains functional [12]. Thus we shall assume $s > 0$. The steady-state population size T_0 should be less than T_{\max} , so that the T-cell population will expand when stimulated, as occurs, say, during infection. Further, if the population ever reaches T_{\max} it should decrease. Thus, we choose

$$\mu_T T_{\max} > s, \quad (4)$$

so that the death rate at T_{\max} is greater than the supply rate. If this were not the case, then the population could increase past T_{\max} . Further, Equations (3) and (4) and the condition $s > 0$ imply that $T_0 < T_{\max}$ as we desire. To see this, note that $f(0) = s > 0$ and $f(T_{\max}) = s - \mu_T T_{\max} < 0$. Thus, all solutions to Equation (1) that begin with an initial number of T cells, $T(0)$, in the interval $I = [0, T_{\max}]$ will remain bounded and stay in the open interval $0 < T(t) < T_{\max}$ for all t . Because T_0 is the only fixed point in I , T_0 is stable and globally attracting in I .

Besides controlling the T-cell population level, Equation (1) has the nice property that the death of T cells can be balanced by the supply of new T cells, the division of T cells in the periphery, or both. Consequently, the net T-cell proliferation rate $p = r - \mu_T$ need not be positive. In the absence of environmental antigen and with little idiotypic network stimulation, one might imagine that r is small or even zero and $p < 0$ but that the total T-cell population is maintained at a positive value through the creation of new T cells. One might also expect that before thymic involution the source s is more important than division in the periphery, so that small or negative values of p could still give positive steady states. After thymic involution, which causes s to decrease, or following adult thymectomy, which causes s to equal zero, one might assume that humoral or growth-factor-regulated control mechanisms ensure that $p > 0$ so as to give a positive steady-state T-cell population size. Thus, the parameter s and possibly the parameter r may vary with age and antigenic experience. These parameter variations could be important in explaining the observed differences in the dynamics of T-cell depletion due to HIV infection in people of different ages [49].

2.2. HIV INFECTION

To model the influence of HIV on T-cell growth, we need to take into consideration a number of features of the life history of the virus [13]. HIV is an RNA virus. However, when it infects a cell, the enzyme reverse transcriptase, which it carries, makes a DNA copy of its RNA genome. This DNA copy is then integrated into the DNA of the infected cell. The viral DNA, called the provirus, is then duplicated with the cell's DNA every time the cell divides. Thus, once infected, a cell remains infected for life. Within a T cell the provirus can remain latent, giving no sign of its presence for months or years [26]. Stimulation of the T cell by antigen or a mitogen can lead to the production of new virus particles that bud from the surface of the infected cell. The budding can take place slowly, sparing the host cell, or it can take place very rapidly, possibly leading to lysis of the T cell [37].

To model these events, we consider T cells that are uninfected, T cells that are latently infected (i.e., that contain the provirus but are not producing it), and T cells that are actively infected (i.e., that are producing virus). We also consider the population of free infectious viral particles. To describe the dynamics of these populations we formulate an ordinary differential equation model. Thus spatial dependence is ignored, and the various interactions are imagined to occur in a well-mixed compartment such as the bloodstream. To correctly account for interactions in the tissues, more complex models involving multiple compartments and/or partial differential equations may be needed. Also, because the model is deterministic, it does not correctly account for the very early stages of the infection nor can it totally account for the variability seen among infected individuals. Some variability can be ascribed to different parameter values being characteristic of different viral strains or different patients.

Let T denote the concentration of uninfected CD4⁺ T cells, and let T^* and T^{**} denote the concentrations of latently infected and actively infected CD4⁺ T cells. The concentration of free infectious virus particles is V . We will not be concerned with noninfectious viral particles. Definitions of the parameters can be found in Table 1. We assume that the dynamics of the various populations are given by

$$\frac{dT}{dt} = s - \mu_T T + rT \left(1 - \frac{T + T^* + T^{**}}{T_{\max}} \right) - k_1 VT, \quad (5a)$$

$$\frac{dT^*}{dt} = k_1 VT - \mu_T T^* - k_2 T^*, \quad (5b)$$

$$\frac{dT^{**}}{dt} = k_2 T^* - \mu_b T^{**}, \quad (5c)$$

$$\frac{dV}{dt} = N\mu_b T^{**} - k_1 VT - \mu_V V. \quad (5d)$$

Equation (5a) is a modified form of (1). Again s is a source term and represents the rate of generation of new (presumably uninfected) CD4⁺ T cells from precursors in the bone marrow and thymus. HIV can infect precursor cells and may have the effect of decreasing the supply of new cells [11]. Thus, in more refined models one may need to consider s as a decreasing function of v . This case is considered in Section 7, in Perelson [49], and in a version of the model of Nowak et al. [48]. Uninfected T cells have a finite life span and are assumed to die at the

TABLE 1
Variables and Parameters

	Initial or default values	
Dependent variables		
T	Uninfected CD4 ⁺ cell population size	1000 mm ⁻³
T^*	Latently infected CD4 ⁺ helper cell population size	0
T^{**}	Actively infected CD4 ⁺ helper cell population size	0
V	HIV population size	10 ⁻³ mm ⁻³
Parameters and constants		
s	Rate of supply of CD4 ⁺ T cells from precursors	10 day ⁻¹ mm ⁻³
r	Rate of growth for the CD4 ⁺ cell population	0.03 day ⁻¹
T_{\max}	Maximum CD4 ⁺ cell population level	1500 mm ⁻³
μ_T	Death rate of uninfected and latently infected CD4 ⁺ cells	0.02 day ⁻¹
μ_b	Death rate of actively infected CD4 ⁺ cell population	0.24 day ⁻¹
μ_V	Death rate of free virus	2.4 day ⁻¹
k_1	Rate constant for CD4 ⁺ cells becoming infected by free virus	2.4 × 10 ⁻⁵ mm ³ day ⁻¹
k_2	Rate latently infected cells convert to actively infected	3 × 10 ⁻³ day ⁻¹
N	Number of free virus produced by lysing a CD4 ⁺ cell	Varies
θ	Viral concentration needed to decrease s to $s/2$	1 mm ⁻³
Derived quantities		
T_0	Steady-state level of CD4 ⁺ cells in uninfected individuals	1000 mm ⁻³
N_{crit}	Critical number of viral progeny needed for endemic infection	774
k_3	$= k_2 + \mu_T$	0.023 day ⁻¹
k_4	$= k_1 T_0 + \mu_V$	2.424 day ⁻¹
\hat{k}_4	$= k_1 \bar{T} + \mu_V$	
γ	$= r / T_{\max}$	2 × 10 ⁻⁵ day ⁻¹
p	$= r - \mu_T$	0.01 day ⁻¹

same rate per cell, μ_T , as in uninfected individuals. In Equation (5b), latently infected T cells are also assumed to have precisely the same natural life span ($\sim 1/\mu_T$), although other factors can augment the natural death rate.

If a T cell encounters the antigen for which it is specific, it may be stimulated to grow. T-cell stimulation is a complex matter. Here we are dealing with T cells of all specificities, and thus we simply assume that a constant fraction of T cells are stimulated to grow. In the mouse,

Freitas et al. [18] find that about 10% of peripheral T cells are activated large cells. In humans the situation may be different. Analyzing peripheral blood lymphocytes (PBLs) of a healthy individual, one typically finds that on the order of 1% of the cells are activated, using the criterion of IL-2 receptor expression (K. Smith, personal communication). Since many of the PBLs with IL-2 receptors may be natural killer cells, fewer than 1% of CD4⁺ T cells may be activated. In a more complex model one can make the fraction of cells stimulated, f_s , a variable in the model and let it be a function of the antigen concentration and possibly other factors such as lymphokines and antigen presentation by macrophages. As the HIV infection progresses, the fraction of cells stimulated may change, so this enhancement may be quite interesting. Here we assume that f_s is a constant and that the parameter r in Equations (1) and (5a) is given by $r = \hat{r}f_s$, where \hat{r} is the average antigen- or idiotypic network-induced per capita T-cell growth rate in the absence of population density limitation.

The other terms in Equations (5a) and (5b) deal with the effects of HIV. The term k_1VT models the rate at which free virus infects a CD4⁺ T cell. A simple mass-action type of term has been used with rate constant k_1 . Once a T cell has been infected, it becomes a latently infected or T* cell; thus k_1VT is subtracted from (5a) and added to (5b).

Equation (5c) models the population dynamics of actively infected T cells. Actively infected cells are presumed to be generated from latently infected cells with rate constant k_2 . This activation event probably involves the latently infected cell being stimulated to divide. In vitro, a variety of stimuli including antigens and mitogens have been shown to induce HIV expression [17, 41]. Thus k_2 , like r , should be a function of antigen concentration and the fraction of cells stimulated by antigen. However, it also includes the probability that stimulation leads to viral production. Active viral replication and budding from these cells is assumed to lead to lysis at rate μ_b [37]. Although actively infected cells may divide once or twice and generate a few daughter cells [37], we feel that this expansion is sufficiently minor that it can be ignored. The major factor that needs to be modeled correctly is the total number of infectious virus particles produced by one infected cell during its lifetime, including any of its daughter cells. We call this quantity N . In this model we treat both μ_b and N as parameters characteristic of a particular viral species. Both parameters, however, may be related to the viral replication rate. One would expect that viral strains with high replication rates would have high values of N . However, the lytic rate μ_b may also depend on the replication rate—viruses with low replication rate may kill poorly, if at all, while those with high replication rates may kill rapidly, say by membrane disruption during viral budding. A

detailed model of these relationships will be presented elsewhere. Here we treat N , μ_b , and other parameters as constants. If slow/low strains are replaced by rapid/high variants, then various parameters, such as N , could be slowly varying (see Section 10).

Equation (5d) models the free infectious virus population. As stated above, we assume that an actively infected $CD4^+$ T cell produces N virus particles. For simplicity, we take the rate of virus production equal to N times the death rate of the cell. For example, this would be the case if the viruses were released upon cell death. Free virus is lost by binding to uninfected $CD4^+$ T cells at rate k_1VT . Binding might also occur to latently infected cells and cause superinfection. Here we neglect this possibility in order to keep the model as simple as possible. Recent measurements using the polymerase chain reaction [55] indicate that in patients with AIDS approximately 1 in 100 cells are latently infected, while in HIV—seropositive patients who are asymptomatic, $< 1/10,000$ – $1/1000$ $CD4^+$ T cells are infected [56]. Thus, neglecting binding to latently infected cells should not introduce much error. Actively infected cells tend to lose their CD4 [27], and hence viral binding to actively infected cells can also be justifiably neglected. The last term in (5d), $-\mu_V V$, accounts for loss of viral infectivity, viral death, and/or clearance from the body.

In the absence of virus, the T-cell population has the steady-state value T_0 . Thus reasonable initial conditions for this system of equations are $T(0) = T_0$, $T^*(0) = 0$, $T^{**}(0) = 0$, and $V(0) = V_0$ for infection by free virus, or $T(0) = T_0$, $T^*(0) = T_0^*$, $T^{**}(0) = T_0^{**}$, $V(0) = V_0$ for infection by both infected cells and virus.

3. ANALYSIS

We first remark that the model is reasonable in the sense that no population goes negative and no population grows unbounded. The nonnegative orthant $R_+^4 = \{x \in R^4 | x \geq 0\}$ is called a positively invariant region if a trajectory that starts in the nonnegative orthant remains there forever. What is needed for this is to show that on each hyperplane bounding the nonnegative orthant the vector field points into R_+^4 . From Equations (5) we find precisely this; that is,

$$\begin{aligned} \left. \frac{dT}{dt} \right|_{T=0} &= s \geq 0, & \left. \frac{dT^*}{dt} \right|_{T^*=0} &= k_1VT \geq 0, \\ \left. \frac{dT^{**}}{dt} \right|_{T^{**}=0} &= k_2T^* \geq 0, & \left. \frac{dV}{dt} \right|_{V=0} &= N\mu_b T^{**} \geq 0. \end{aligned}$$

One of the properties of the logistic equation for T-cell growth, Equation (1), is that if $T(0) < T_{\max}$, then $T(t) < T_{\max}$ for all t . Since the

presence of HIV only decreases the T-cell population, this property should remain true for $T_{\text{tot}} = T + T^* + T^{**}$. To prove this we show that $(dT_{\text{tot}}/dt)|_{T_{\text{tot}}=T_{\text{max}}} < 0$. From Equations (5a)–(5c) we see that

$$\frac{dT_{\text{tot}}}{dt} = s - \mu_T T + rT \left(1 - \frac{T_{\text{tot}}}{T_{\text{max}}}\right) - \mu_T T^* - \mu_b T^{**}.$$

Death by viral cytopathicity occurs faster than death by natural means; that is, $\mu_b > \mu_T$. Therefore,

$$\frac{dT_{\text{tot}}}{dt} < s - \mu_T T_{\text{tot}} + rT \left(1 - \frac{T_{\text{tot}}}{T_{\text{max}}}\right).$$

Hence at $T_{\text{tot}} = T_{\text{max}}$,

$$\left. \frac{dT}{dt} \right|_{T_{\text{tot}}=T_{\text{max}}} < s - \mu_T T_{\text{max}} < 0.$$

The last inequality follows from Equation (4). Thus, in the case of HIV infection, the total T-cell population, T_{tot} , and hence the various subpopulations, $T(t)$, $T^*(t)$, and T^{**} , are all bounded by T_{max} .

We now show that within the nonnegative orthant there are two possible steady states, one with no virus present, an *uninfected steady state*, and another with a constant level of virus, an *endemically infected steady state*. Setting the left-hand sides of Equations (5b) and (5c) to zero yields

$$T^* = \frac{k_1 VT}{k_2 + \mu_T}, \quad (6)$$

$$T^{**} = \frac{k_2 T^*}{\mu_b} = \frac{k_2 k_1 VT}{\mu_b (k_2 + \mu_T)}. \quad (7)$$

Substituting Equations (6) and (7) into (5d), one finds

$$\frac{dV}{dt} = \left[\left(\frac{Nk_2}{k_2 + \mu_T} - 1 \right) k_1 T - \mu_V \right] V. \quad (8)$$

The equation $dV/dt = 0$ has two possible solutions, $V = 0$ and $T = \mu_V/\alpha$, where

$$\alpha = k_1 \left(\frac{Nk_2}{k_2 + \mu_T} - 1 \right). \quad (9)$$

If $V = 0$, then from (6) and (7), $T^* = T^{**} = 0$. Substituting into (5a), we find quite obviously that there exists one steady state in which the

virus is totally absent. We call this the *uninfected state*. It is given by

$$\bar{T} = T_0, \quad \bar{T}^* = \bar{T}^{**} = \bar{V} = 0, \quad (10)$$

where an overbar denotes a steady-state value and T_0 is given by Equation (3). Introducing the parameters

$$p = r - \mu_T \quad \text{and} \quad \gamma = r/T_{\max}, \quad (11a,b)$$

we can rewrite (3) in a form that will be useful later:

$$T_0 = \frac{p + \sqrt{p^2 + 4s\gamma}}{2\gamma}. \quad (12)$$

If $V \neq 0$, then substituting $T = \mu_V/\alpha$ and Equations (6) and (7) into Equation (5a) leads to a second steady state, which we call the *endemi- cally infected state*. In this state,

$$\bar{T} = \mu_V/\alpha = \frac{\mu_V k_3}{k_1(Nk_2 - k_3)}, \quad (13a)$$

$$\bar{T}^* = \frac{k_1 \mu_V \bar{V}}{\alpha k_3} = \frac{\mu_V \bar{V}}{Nk_2 - k_3}, \quad (13b)$$

$$\bar{T}^{**} = \frac{k_2 k_1 \mu_V \bar{V}}{\mu_b \alpha k_3} = \frac{k_2 \mu_V \bar{V}}{\mu_b(Nk_2 - k_3)}, \quad (13c)$$

$$\bar{V} = \frac{s\alpha^2 + p\alpha\mu_V - \gamma\mu_V^2}{k_1 \mu_V(\alpha + \beta\mu_V)}, \quad (13d)$$

where

$$k_3 = k_2 + \mu_T, \quad \beta = \frac{\gamma}{k_3} \left(1 + \frac{k_2}{\mu_b}\right). \quad (14)$$

3.1. STABILITY OF THE UNINFECTED STATE

For the uninfected steady state to be asymptotically stable we require that after the introduction of a small amount of virus, $dV/dt < 0$. Setting $T = T_0$ and examining (8), we find $dV/dt < 0$ if and only if $N < N_{\text{crit}}$, where

$$N_{\text{crit}} = \frac{k_3(\mu_V + k_1 T_0)}{k_2 k_1 T_0}. \quad (15)$$

Thus, a reasonable conjecture is that the uninfected steady state is stable if and only if $N < N_{\text{crit}}$. This is formally proved below.

The Jacobian matrix \mathbf{A} for system (5) evaluated at the uninfected steady state is given by

$$\mathbf{A} = \begin{pmatrix} -a & -\gamma T_0 & -\gamma T_0 & -k_1 T_0 \\ 0 & -k_3 & 0 & k_1 T_0 \\ 0 & k_2 & -\mu_b & 0 \\ 0 & 0 & N\mu_b & -k_4 \end{pmatrix}, \quad (16)$$

where

$$k_4 = k_1 T_0 + \mu_\nu, \quad a = -p + 2T_0\gamma. \quad (17)$$

Substituting the value of T_0 from Equation (12), one sees that $a = \sqrt{p^2 + 4s\gamma} > 0$.

The uninfected steady state is asymptotically stable if and only if all of the eigenvalues of the Jacobian matrix \mathbf{A} have negative real parts. The eigenvalues can be determined by solving the characteristic equation $\det(\mathbf{A} - \lambda\mathbf{I}) = 0$. For \mathbf{A} given by Equation (16), this becomes

$$(\lambda + a)[(\lambda + \mu_b)(\lambda + k_3)(\lambda + k_4) - k_1 k_2 T_0 N \mu_b] = 0, \quad (18)$$

and hence one eigenvalue is $\lambda = -a < 0$. Dividing Equation (18) by $\lambda + a$, we obtain the reduced equation

$$\lambda^3 + A\lambda^2 + B\lambda + C = 0, \quad (19)$$

where the coefficients

$$A = \mu_b + k_3 + k_4 > 0, \quad (20a)$$

$$B = k_3 k_4 + \mu_b(k_3 + k_4) > 0, \quad (20b)$$

$$C = \mu_b(k_3 k_4 - k_1 k_2 T_0 N). \quad (20c)$$

Using the definition of N_{crit} , we can rewrite Equation (20c) as

$$C = \mu_b k_1 k_2 T_0 (N_{\text{crit}} - N). \quad (20d)$$

By the Routh-Hurwitz criteria [63], the three roots of the characteristic equation (19) will have negative real parts if and only if

$$A, C > 0 \quad \text{and} \quad AB - C > 0.$$

The coefficient A is the sum of positive terms and is positive. Under the condition $N < N_{\text{crit}}$, we have $C > 0$ and

$$\begin{aligned} AB - C &= \mu_b^2(k_3 + k_4) + \mu_b(k_3^2 + k_4^2 + 2k_3 k_4 + k_1 k_2 T_0 N) \\ &\quad + k_3 k_4(k_3 + k_4) > 0. \end{aligned}$$

Thus, if $N < N_{\text{crit}}$, the uninfected state is asymptotically stable.

If $N = N_{\text{crit}}$, $C = 0$, and (19) then implies that one eigenvalue must be zero. Applying the Routh-Horowitz condition to the reduced characteristic polynomial $\lambda^2 + A\lambda + B$, it is easy to see that the remaining two eigenvalues have negative real part. Thus, if $N = N_{\text{crit}}$, the uninfected state is neutrally stable.

If $N > N_{\text{crit}}$, then by (20d) $C < 0$, and thus at least one eigenvalue will have positive real part. When $C < 0$ there is one sign change in (19). Hence by Descartes' rule of signs [44] we can conclude that there is exactly one positive eigenvalue when $N > N_{\text{crit}}$. Thus, the uninfected state is unstable if $N > N_{\text{crit}}$.

These results imply that for the uninfected steady state, N is a bifurcation parameter and that the stability of the state is lost as N increases past N_{crit} (Figure 1).

So far, we have dealt with only the local stability of the uninfected steady state. For $N < N_{\text{crit}}$ there is only one steady state in the nonnegative orthant, and we conjecture that it is globally stable. For $0 \leq N < (k_2 + \mu_T)/k_2 < N_{\text{crit}}$, it is easy to show that this conjecture is true. Consider the function $L(t) = T^* + NT^{**} + V$, which as we shall see is a

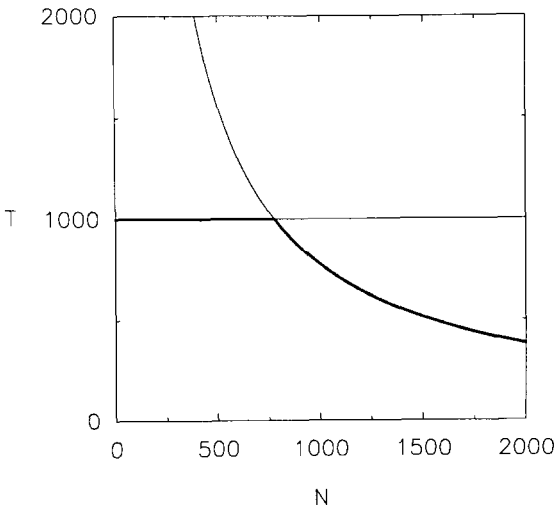


FIG. 1. Transcritical bifurcation. The steady-state values of T are plotted versus N . Stable steady states are indicated by dark heavy lines, unstable steady states by light lines. Parameter values are given in Table 1. For $N < N_{\text{crit}} = 774$, the uninfected steady state with $T = 1000$ is stable. At $N = N_{\text{crit}}$ this state loses its stability, and the endemically infected state with T a decreasing function of N becomes stable.

Lyapunov function. In the nonnegative orthant, $L(t) \geq 0$. From Equations (5),

$$\frac{dL}{dt} = [(N-1)k_2 - \mu_T]T^* - \mu_V V.$$

For $N < (k_2 + \mu_T)/k_2$, the term in brackets is negative, and hence $dL/dt < 0$. Thus, as $t \rightarrow \infty$, $L(t) \rightarrow 0$. Hence T^* , T^{**} , and V all approach 0, and $T \rightarrow T_0$.

3.2. ENDEMICALY INFECTED STEADY STATE

At $N = N_{\text{crit}}$, $\alpha = \mu_V / T_0$ and $\bar{V} = 0$. This can be seen by substituting (15) into (9) and then substituting μ_V / T_0 for α in (13d). Thus, at $N = N_{\text{crit}}$, the endemically infected state and the uninfected state coincide. At $N = N_{\text{crit}}$, there is a transcritical bifurcation, and the endemically infected state emerges for $N > N_{\text{crit}}$ as a new steady state in R_+^4 . For $N < N_{\text{crit}}$, the infected steady state does not lie in R_+^4 , because $\bar{V}, \bar{T}^*, \bar{T}^{**} < 0$, and hence it is unphysical. Further, since R_+^4 is positively invariant, this unphysical steady state is not reachable from initial conditions in R_+^4 . Thus, we need only study the stability of the endemically infected state for $N > N_{\text{crit}}$.

Linearizing Equations (5) around the endemically infected state, we obtain the Jacobian matrix \mathbf{A} ,

$$\mathbf{A} = \begin{pmatrix} -a & -\gamma\bar{T} & -\gamma\bar{T} & -k_1\bar{T} \\ k_1\bar{V} & -k_3 & 0 & k_1\bar{T} \\ 0 & k_2 & -\mu_b & 0 \\ -k_1\bar{V} & 0 & N\mu_b & -\hat{k}_4 \end{pmatrix}, \quad (21)$$

where

$$k_3 = k_2 + \mu_T, \quad (22a)$$

$$\hat{k}_4 = k_1\bar{T} + \mu_V, \quad (22b)$$

$$a = -p + \gamma(2\bar{T} + \bar{T}^* + \bar{T}^{**}) + k_1\bar{V}, \quad (22c)$$

and \bar{T} , \bar{T}^* , \bar{T}^{**} , and \bar{V} are given by Equations (13). Using the steady state form of (5a),

$$0 = s + p\bar{T} - \gamma\bar{T}(\bar{T} + \bar{T}^* + \bar{T}^{**}) - k_1\bar{V}\bar{T},$$

one easily sees $a\bar{T} = s + \gamma\bar{T}^2$, and hence

$$a = \gamma\bar{T} + s/\bar{T} > 0. \quad (23)$$

Examining the characteristic polynomial, $\det(\mathbf{A} - \lambda\mathbf{I})$, we find it has the form $\lambda^4 + b\lambda^3 + c\lambda^2 + d\lambda + e$, where the coefficients are

$$b = a + k_3 + \hat{k}_4 + \mu_b > 0, \quad (24a)$$

$$c = a(k_3 + \hat{k}_4 + \mu_b) + \mu_b(k_3 + \hat{k}_4) + k_3\hat{k}_4 + k_1\bar{T}\bar{V}(\gamma - k_1), \quad (24b)$$

$$d = a[k_3\hat{k}_4 + \mu_b(k_3 + \hat{k}_4)] + k_1\bar{V}\bar{T}[\gamma(\mu_V + k_2 + \mu_b) - k_1(k_3 + \mu_b)], \quad (24c)$$

$$e = k_1\bar{V}\bar{T}[k_1\mu_b(Nk_2 - k_3) + \gamma\mu_V(k_2 + \mu_b)]. \quad (24d)$$

In calculating the coefficients of the characteristic polynomial we have eliminated a term proportional to $k_3\hat{k}_4 - k_1k_2\bar{N}\bar{T}$ from both d and e , because substituting the definitions of \hat{k}_4 and \bar{T} shows that this term is zero.

Analyzing the characteristic polynomial, it is obvious that b is positive. For $N > N_{\text{crit}}$, $Nk_2 > k_3$. Thus e is positive as well.

To establish the stability of this steady state, it is also necessary to show that both c and d are positive and that $(bc - d)/d/b^2 > e$. For the parameters given in Table 1, all three conditions are met; however, for some parameter regimes, this steady state is unstable (Table 2).

4. T-CELL DEPLETION

In the endemically infected state, normal T cell population regulation is disturbed by the presence of HIV. In this new steady state the

TABLE 2
Parameters for Oscillations

	Parameters and constants	Initial or default value
s	Rate of supply of CD4 ⁺ T cells from precursors	10 day ⁻¹ mm ⁻³
r	Rate of growth for the CD4 ⁺ cell population	12 day ⁻¹
T_{max}	Maximum CD4 ⁺ cell population level	1500 mm ⁻³
μ_T	Death rate of uninfected and latently infected CD4 ⁺ cells	0.06 day ⁻¹
μ_b	Death rate of actively infected CD4 ⁺ cell population	0.24 day ⁻¹
μ_V	Death rate of free virus	5 day ⁻¹
k_1	Rate constant for CD4 ⁺ cells becoming infected by free virus	2.4 mm ³ day ⁻¹
k_2	Rate latently infected cells convert to actively infected	1.2 × 10 ⁻⁴ day ⁻¹
N	Number of free virus produced by lysing a CD4 ⁺ cell	1200

T-cell level can be considerably lower than in the uninfected steady state. Thus, one of the main conclusions of this model is that HIV infection itself may be sufficient to account for a substantial amount of the T-cell depletion seen in AIDS. To establish under what conditions this is the case, we examine Equation (11) in some detail.

As a simplifying approximation let us assume that with appropriate parameter choices the model can mimic the population distribution in vivo in which, say, 1 in 100 cells are latently infected and 1 in 10,000 to 1 in 100,000 are actively infected. In this case, T-cell depletion must occur predominantly in the uninfected pool. According to (13a), at steady state the uninfected T-cell population size is

$$\bar{T} = \frac{\mu_V}{k_1(Nk_2/k_3 - 1)},$$

where $k_3 = k_2 + \mu_T$. Since $N > N_{\text{crit}}$, let $N = N_{\text{crit}} + n$. Then, substituting the value of N_{crit} from Equations (15), one can write

$$\frac{\bar{T}}{T_0} = \frac{1}{1 + \delta}, \quad (25)$$

where

$$\delta = \frac{k_1 n T_0}{\mu_V (\mu_T / k_2 + 1)}. \quad (26)$$

Since $\delta > 0$, $\bar{T} < T_0$, and there is depletion of uninfected cells at the endemically infected steady state. As a useful measure of the degree of depletion of uninfected cells, we introduce

$$D = 1 - (T/T_0) = \delta / (1 + \delta). \quad (27)$$

Thus, $D = 0$ implies no depletion and $D = 1$ means total depletion. The larger δ , the larger the depletion. Consequently, there is increased depletion of uninfected T cells

- (1) If the virus lives longer (i.e., if μ_V is decreased).
- (2) If there is a higher rate of viral infection (i.e., if k_1 is increased).
- (3) If a larger number of viruses are produced per T cell (i.e., if n is increased).

Further, if $\mu_T / k_2 \gg 1$, then there is also increased depletion

- (1) If there is more rapid conversion from the latent to the actively infected state (i.e., if k_2 is increased), or
- (2) If T cells live longer (i.e., if μ_T is decreased).

We also note that the depletion of uninfected cells is independent of μ_b , the death rate of actively infected cells, and s , the rate of supply of uninfected cells. However, increasing μ_b will have a small effect on the total T-cell population because it will decrease T^{**} . Also, increasing s will increase V and thus, from (13b) and (13c), increase T^* and T^{**} . Thus, as one would expect, increasing s will decrease the total depletion. To see this explicitly, we compute the steady-state level of infected cells. From Equations (13b–13d) and (14) we find

$$\bar{T}^* + \bar{T}^{**} = \frac{\beta [s\alpha^2 + p\alpha\mu_V - \gamma\mu_V^2]}{\gamma\alpha(\alpha + \beta\mu_V)}, \quad (28)$$

where α , β , and γ , given by Equations (9), (10), and (14), are independent of s .

5. PARAMETER VALUES

Choosing parameter values characteristic of the *in vivo* situation is difficult; many of the parameters in our model have not been measured, or, if measurements have been attempted, they may not be as accurate as we need for quantitative predictions. Thus one role of modeling is to point out where further quantitative measurements can improve our understanding of the AIDS disease process.

The number of CD4⁺ T cells in the peripheral blood is approximately 1000/mm³, although it fluctuates both diurnally and with the total lymphocyte count [33, 34, 40]. We shall choose 10³ as the “standard” number of CD4⁺ T cells (per mm³) in a healthy individual and use this value as an initial condition, $T_0 = T(0) = 10^3$. As is common in the clinical literature, we shall report all T-cell numbers per cubic milliliter. The T-cell number in the blood fluctuates and can easily increase by 50% or so [1]. Thus we choose $T_{\max} = 1.5 \times 10^3$, which is higher than typically reported T4 counts in healthy individuals but lower than the maximum that can be obtained in severe infection. Under conditions of infection, different lymphokines are secreted and different control mechanisms presumably come into play. Under such conditions our model of T-cell population dynamics would have to be modified. Our assumption of a noninfectious situation is consistent with the modeling approach taken here in which the immune response to HIV and other antigens is being neglected.

We assume that activated T cells divide every 12–18 h. Therefore the growth rate of an activated cell is approximately 1 day⁻¹. This growth rate must be multiplied by the fraction of T cells that are dividing. This is probably on the order of 1%. To this is added a death rate, so that r

represents the net rate of increase in the population when cell death is taken into account. In the simulations reported here, we let $r = 0.03 \text{ day}^{-1}$, $\mu_T = 0.02 \text{ day}^{-1}$ (see below), and hence the net proliferation rate $p = 0.01 \text{ day}^{-1}$. Smaller growth and death rates would also be reasonable.

The lifetime of unactivated T cell is variable. Memory cells may live a long time, whereas precursor cells and non-memory T cells may live a short time. Freitas et al. [18] report that 50–60% of peripheral mature T lymphocytes of the mouse are replaced every 2–3 days. In this model, where we have not distinguished subpopulations of T cells, the death rate μ_T represents an average over all subpopulations. Thus, although some human T cells may live for years, it is clear that many T cells have much shorter lifetimes. Recent work of Gray [22] and Gray and Leanderson [23] indicates that memory T cells may live 2–6 weeks in the absence of antigen-stimulated replication. This we feel is reasonable as an average. Thus we take $\mu_T = 0.02 \text{ day}^{-1}$, which corresponds to a half-life of 36 days.

The supply of new T cells from precursors populations must be less than the number required to maintain the T-cell population constant. Thus $s \leq \mu_T T_0$. With $T_0 = 10^3 \text{ mm}^{-3}$ and μ_T as above, $s \leq 20 \text{ day}^{-1} \text{ mm}^{-3}$. If we take $s = 10 \text{ day}^{-1} \text{ mm}^{-3}$, with r as given above, half of the T-cell replenishment is by proliferation in the periphery and half from the supply term. The parameters r , s , and μ_T have been chosen so that, in the absence of virus, the population of CD4⁺ T cells is maintained at its initial value $T_0 = 10^3 \text{ mm}^{-3}$. Other choices of these parameters, of course, can also maintain this steady-state population level.

Estimating the rate k_1 at which virus infects T cells is difficult. Because k_1 is a bimolecular rate constant, it has the dimensions of 1 over cell concentration per unit time. A useful scaling is therefore to consider $k_1 T_0$, which has the units of time^{-1} . In order for a virus to infect a cell, it must encounter the cell, bind CD4 or some other receptor, and then enter the cell. Thus infection cannot be any faster than the rate of transport to the cell surface. We can thus use Smoluchowski's formula for the diffusion-limited rate constant to provide an upper bound on k_1 . For interaction between two spherical particles of radii r_T and r_V and diffusion coefficients D_T and D_V , $k_1 \leq 4\pi(r_T + r_V)(D_T + D_V)$. Using $r_V = 5 \times 10^{-6} \text{ cm}$, $r_T = 4 \times 10^{-4} \text{ cm}$, $D_V = 2 \times 10^{-8} \text{ cm}^2 \text{ s}^{-1}$, and $D_T = 2.5 \times 10^{-10} \text{ cm}^2 \text{ s}^{-1}$ as given in Layne et al. [36], $k_1 \leq 10^{-10} \text{ cm}^3 \text{ s}^{-1} = 0.6 \times 10^{-3} \text{ mm}^3 \text{ h}^{-1}$. Hence $k_1 T_0 \leq 0.36 \text{ h}^{-1}$. For particles the size of HIV, convective transport would not be able to increase this rate [52]. Once a virus particle encounters a cell, it need not infect it. The CD4 level will vary among T cells. Cells with low levels of CD4 may resist infection. Further, the state of activation of the

cell may be important. Some work has suggested that only activated T cells can be successfully infected [21, 65]. Kiernan et al. [31], using an in vitro system, found that although 40% of input virus attached to cells, only 2–3% of cells became actively infected. Thus, it seems reasonable to suppose that only a fraction of the encounters between HIV and T cells will lead to infection. As an initial guess, we assume that $k_1 T_0 = 10^{-3} \text{ h}^{-1} = 2.4 \times 10^{-2} \text{ days}^{-1}$. Since different viral strains have different tropisms and different degrees of virulence, one might safely assume that k_1 is a strain-dependent parameter that can vary greatly.

Latently infected cells behave the same as normal T cells and thus should have the same death rate. However, we assume that when they interact with antigen, rather than dividing they become actively infected. The time for death of an actively infected cell is probably a few days to a week. Somasundaran and Robinson [57] found that in cells of the T-cell line C8166, a 3–4-day lag occurred between expression of viral proteins and cell death in actively infected cells. Kiernan et al. [31] found that HIV-infected MT-2 cells remain viable up to 62 h postinfection, after which viability rapidly decreases. Thus we shall choose $\mu_b = 0.24 \text{ day}^{-1}$.

The number of infectious viruses released, N , is not known precisely. Merrill [42] suggests that N is between 50 and 1000. Layne et al. [36] estimate $N > 300$ from data on the minimum concentration of soluble CD4 needed to block HIV infectivity in an in vitro assay. Somasundaran and Robinson [57] find that the standard laboratory strain of HIV, IIIB, selected to grow well in culture, can produce between 300,000 and 2.5 million copies of viral RNA in actively infected cells. The number of these viral RNAs that are packaged into viral particles and released was not measured, but such high levels of expression indicate that values of N well above 10^3 are possible. Viral isolates exhibit great variability; some replicate fast and are highly cytopathic, while others replicate slowly [6, 15]. In order to study the differences in disease course with different viral strains we will vary N in our studies. However, we keep N in the low range of permissible values because this model is applicable only to strains of HIV that do not stimulate an immune response. As argued elsewhere, we believe that such strains should be low viral producers [46].

Free virus loses its infectivity over time, probably due to the shedding of gp120 [19]. For example, in a viral infectivity assay, HIV-1 strains IIIB and RFII lost half of their infectivity in 4–6 h at 37°C [36]. Thus we take $\mu_v = 2.4 \text{ day}^{-1}$.

The rate of conversion of a latently infected cell to an actively infected cell is k_2 . We assume that only those latently infected T cells that recognize and respond to the antigen activate HIV replication.

Thus, as in the calculation of the average T-cell growth rate r , k_2 has embedded in it a factor proportional to the average fraction of T cells stimulated by environmental antigen. Because the process of activating HIV replication requires cell division, we expect $k_2 \leq r$. Further, the conversion process may not be 100% efficient; that is, some latently infected cells that are activated by antigen may not produce virus or may produce defective virus. Thus, k_2 may be considerably smaller than r . Here we choose $k_2 = 0.1r = 3 \times 10^{-3} \text{ day}^{-1}$, where the value of r is our default value for healthy individuals responding to normal environmental antigens. If one focuses on times of infection by disease-causing agents other than HIV, the parameters r and hence k_2 could change. Models by Cooper [7], Intrator et al. [30], Reibnegger et al. [54], McLean [41], McLean and Kirkwood [39], Anderson [3], and Anderson and May [4] all consider the effects of secondary infection. Here we are modeling the course of HIV on a long time scale, and the specific effects of one infection or another are not explicitly considered. Rather the net effect of all such antigen encounters is used to estimate the value of r .

A summary of the parameter values used in this paper is given in Table 1. However, other sets of parameters can be used that give similar behavior. If we require that T-cell dynamics in the absence of virus give a steady-state value of 1000 T cells/mm³, then only certain combinations of r , s , T_{\max} , and μ_T are permissible. Once these parameters are established, there is a restricted set of viral parameters that give rise to the long incubation period characteristic of HIV infection. In Perelson [49] the parameters used were quite different ($s = 36 \text{ day}^{-1} \text{ mm}^{-3}$, $r = 0.108 \text{ day}^{-1}$, $\mu_T = 0.072 \text{ day}^{-1}$, $T_{\max} = 1500 \text{ mm}^{-3}$, $k_1 = 2.4 \times 10^{-2} \text{ mm}^3 \text{ day}^{-1}$, $k_2 = 1.2 \times 10^{-4} \text{ day}^{-1}$, $\mu_V = 2.4 \text{ day}^{-1}$, and $\mu_b = 1.2 \text{ day}^{-1}$), yet gave similar dynamical behavior.

6. NUMERICAL SOLUTIONS

To study the time course of the infection, we numerically integrated Equations (5). In Figure 2 we illustrate typical solutions for three values of N all greater than N_{crit} , using the parameters given in Table 1. We choose initial conditions characteristic of an uninfected individual; $T(0) = T_0$, $T^*(0) = T^{**}(0) = 0$, infected with free virus, $V(0) = V_0$. Here we considered the case of exposure to one infectious virion per milliliter, which corresponds to $V_0 = 10^{-3} \text{ mm}^{-3}$. For the parameters in Table 1, $N_{\text{crit}} = 774$. For the three values of N displayed, we see from the upper right panel that the disease is characterized by a lag phase in which there is no discernible T-cell depletion, followed by a phase in which the CD4⁺ T cells decline (Figure 3). In the case $N = 1000$, the lag is about

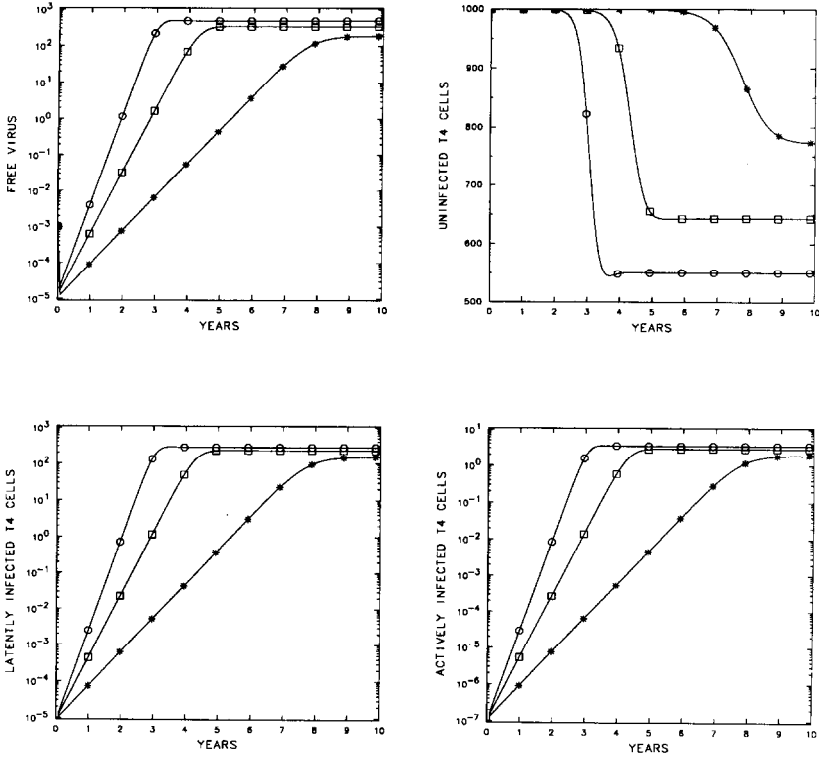


FIG. 2. Dynamics of HIV infection. Solutions of Equations (5a)–(5d). Parameters are given in Table 1. In each graph the three curves correspond to different values of N , the number of infectious virus particles produced per actively infected cell. Here $N_{\text{crit}} = 774$ and $N = 1000$ (*), $N = 1200$ (\square), and $N = 1400$ (\circ).

6 years, with the T-cell decline occurring between years 6 and 8. For larger values of N , the decline in both uninfected and total CD4^+ cells is more substantial but the lag is shorter. The two lower panels in Figure 2 indicate the changes in the latently infected T^* and actively infected T^{**} populations. The curves are essentially identical, up to a scale factor, as might be expected from the establishment of a quasi-steady state in which $dT^{**}/dt = 0$. In a quasi-steady state, Equation (5c) predicts that $T^{**} = k_2 T^* / \mu_b$. Figure 2 shows that such a quasi-steady state is established, because $k_2 / \mu_b = 1.25 \times 10^{-2}$ is the ratio of T^{**} to T^* seen at long times. The number of actively infected cells remains less than 10^{-1} mm^{-3} for 2–5 years depending on N . At this level of expression, less than 1 in 10^4 T cells would be actively infected, as has been observed. Late in the infection process, however, one can

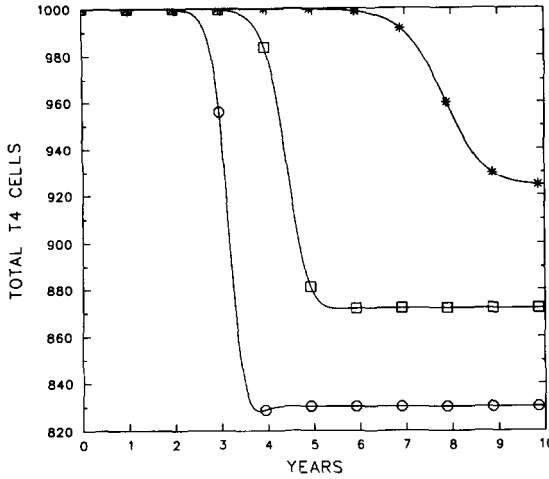


FIG. 3. The total CD4⁺ T-cell population given by $T + T^* + T^{**}$ versus time after infection. The three curves correspond to different values of N , the number of infectious virus particles produced per actively infected cell, $N = 1000$ (*), $N = 1200$ (□), $N = 1400$ (○).

obtain ratios closer to 1 in 100. The number of latently infected cells remains small but increases over time during the initial phase of infection, consistent with measurements of the increasing viral burden in asymptomatic HIV-seropositive patients [56]. The number of latently infected cells ultimately grows to approximately 10^2 mm^{-3} , which is about tenfold larger than the 1 in 100 infected T4 cells observed by Schnittman et al. [55] in patients with AIDS.

The upper left panel in Figure 2 shows the changes in the HIV population. For all three values of N , after a fast initial decline due to cellular binding, the viral population grows exponentially, slowing as its steady-state value of a few hundred virions per cubic millimeter is approached. Comparing the dynamics of viral growth with that of the latently infected and actively infected T-cell populations shows that $V(t)$ follows essentially the same dynamics as the infected T cells. Thus, a quasi-steady-state approximation could again be used with benefit. We return to this point later. Figure 4 shows the change in the free virus population as N is decreased further. If $N < N_{\text{crit}}$, then after the initial binding $V(t)$ decreases exponentially indicating that the infection will not cause disease and that the uninfected state is being approached. With $N > N_{\text{crit}}$, the virus grows after the initial decline, whereas with $N = N_{\text{crit}}$ the virus rapidly attains a constant level and no T-cell depletion is seen (not shown).

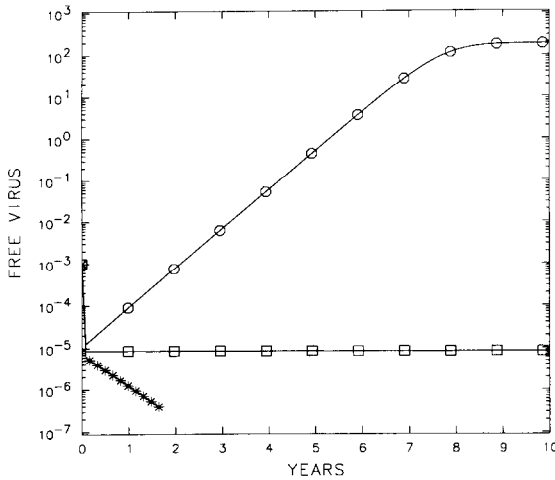


FIG. 4. The change in free virus population for different values of N . Parameters are given in Table 1. For $N < N_{\text{crit}} = 774$, that is, $N = 600$ (*), the virus decays and the system returns to the uninfected state. For $N > N_{\text{crit}}$, that is, $N = 1000$ (\circ), the virus grows, whereas at $N = N_{\text{crit}}$ (\square) the virus remains constant.

Changing the parameters in the model changes the details of the dynamics. For example, increasing N gives rise to larger amounts of T-cell depletion, which is more characteristic of AIDS, but also speeds up the depletion, which is less characteristic (Figure 5). Earlier, we predicted that increased depletion would also occur if μ_V were decreased, that is, if infective virus lived longer. This is what we see in Figure 6. Changing the initial conditions affects the time from infection to depletion. As shown in Figure 7, depletion is noticeable once $V(t)$ reaches a level of about 50 mm^{-3} . Thus, as expected, increasing V_0 decreases the time to depletion. Similar effects are seen if infected cells are used as initial conditions rather than free virus.

6.1. OSCILLATIONS

When the infected steady state is in the positive orthant, that is, for $N > N_{\text{crit}}$, it is also stable for most parameter values of biological interest. In parameter regimes where the infected state is unstable, the system undergoes sustained oscillations around the infected state. We studied the behavior of the system in these regimes by numerical integration, using GRIND [8], and by numerical bifurcation, using AUTO [9]. The parameter regime for oscillations is necessarily different from that in Table 1. Table 2 gives the default parameters used in our study of oscillations. Figure 8 illustrates the dynamics of the system

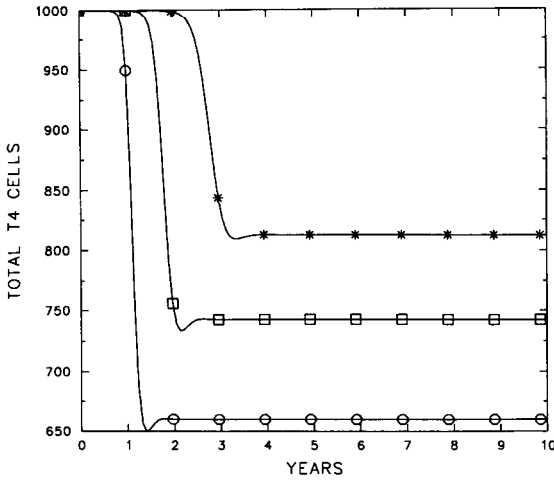


FIG. 5. The degree of T-cell depletion depends upon N . Parameters are given in Table 1. $N = 1500$ (*), $N = 2000$ (\square), and $N = 3000$ (\circ) are shown. As N increases, the depletion increases but the time until depletion decreases.

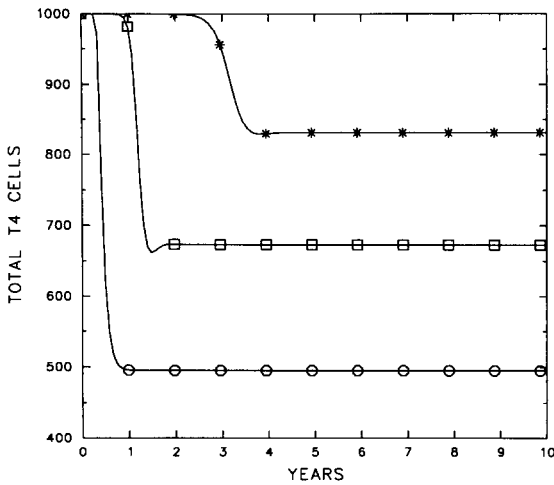


FIG. 6. The influence of the viral death rate μ_V on T-cell depletion. Parameters are given in Table 1; $N = 1400$, $\mu_V = 2.4 \text{ day}^{-1}$ (*), 1.2 day^{-1} (\square), and 0.24 day^{-1} (\circ).

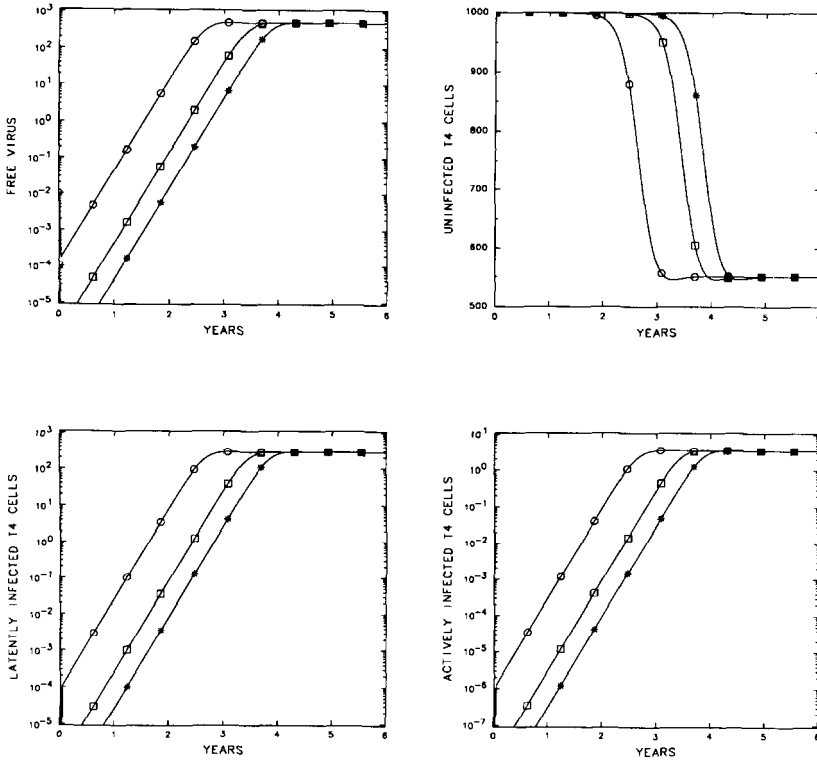


FIG. 7. The effect of changing the initial viral load. Parameters are given in Table 1; $N = 1400$, $V_0 = 10^{-6}$ (*), 10^{-4} (\square), and 10^{-2} (\circ) mm^{-3} .

using the parameters in Table 2. The effects of changing the parameters r , k_1 , and μ_T , which are all quite different than in Table 1, were studied using AUTO. All parameters were set at the default values given in Table 2 except N . Examining Figure 9 for the transcritical bifurcation [62] obtained with these parameters, one notes that the endemically infected state that became stable at $N = N_{\text{crit}} = 502$ loses its stability at a slightly larger value of N and then regains its stability at $N \approx 1229$. Oscillations arise via a Hopf bifurcation when the endemically infected state becomes unstable (light curve in Figure 9). In order to determine the boundary in parameter space for oscillations, we trace one of the two Hopf bifurcations (the upper one at $N = 1229.34$), varying r and μ_T simultaneously in Figure 10a. The region in which oscillations are found is indicated. At the boundaries of the region, the endemically infected steady state changes stability via a Hopf bifurcation. Thus, for example, for $\mu_T = 0.1 \text{ day}^{-1}$ at $r = 1.04$, there is a Hopf bifurcation giving birth to

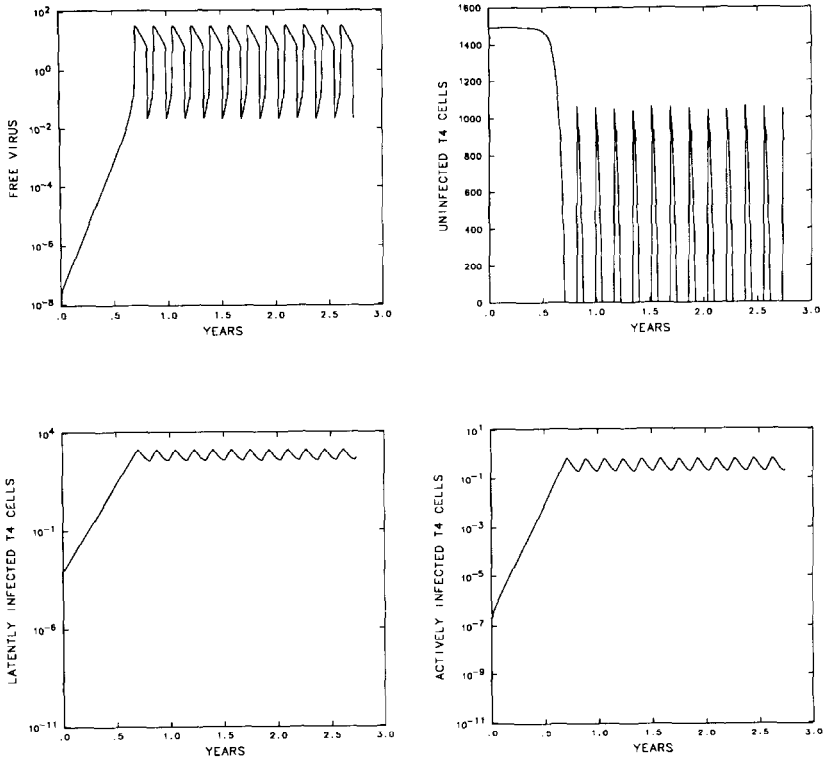


FIG. 8. Dynamics of the system with parameters set in the oscillatory region given in Table 2.

a stable limit cycle. For smaller values of r the infected steady state is stable. If one fixes r , say, at $r = 10 \text{ day}^{-1}$, and varies μ_T , one finds that for small values of μ_T the infected state is stable; it then loses stability by a Hopf bifurcation at $\mu_T \approx 6.1 \times 10^{-2}$ and then goes stable again via a second Hopf bifurcation at $\mu_T \approx 0.146$. Thus, there are two stable regions for the infected steady state, and in between lies a region of oscillatory behavior.

Because k_1 is also important in determining the stability of the endemically infected state, we trace the Hopf bifurcations, varying k_1 and μ_T simultaneously (Figure 10b), and k_1 and r simultaneously (Figure 10c). As in Figure 10a, the curves in these diagrams delimit the region where we find oscillatory behavior from the region where the infected state is stable. We have also studied the size of the region with oscillatory behavior as a function of the other parameters. First, if parameters that are part of N_{crit} are changed such that N_{crit} is increased

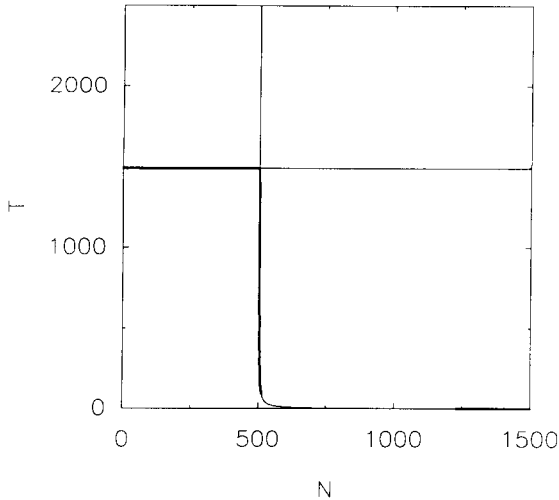
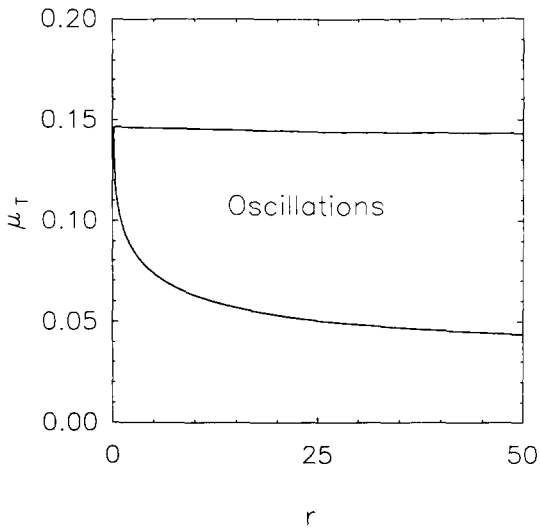


FIG. 9. Transcritical bifurcation. The steady-state values of T are plotted versus N . Stable steady states are indicated by dark heavy lines, unstable steady states by light lines. Parameter values are given in Table 2. For $N < N_{\text{crit}} = 502$, the uninfected steady state with $T = 1000$ is stable. At $N = N_{\text{crit}}$, this state loses its stability and the endemically infected state with T a decreasing function of N becomes stable. This state quickly loses its stability at a Hopf bifurcation and then regains stability at a second Hopf bifurcation at $N = 1229.34$.

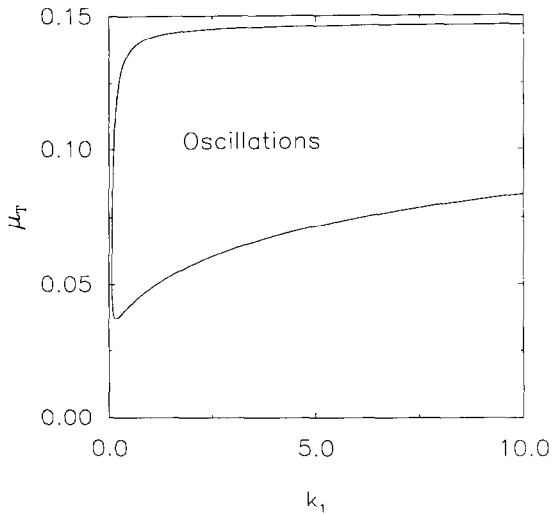
to the point $N < N_{\text{crit}}$, the uninfected state will become stable via the transcritical bifurcation and oscillations will cease. This is, for instance, the case for large values of μ_V and μ_T . Second, changing parameters may increase or decrease the size of the region with oscillatory behavior. Since this region may shrink and disappear entirely as a function of the other parameters, they are as important as k_1 , r , and μ_T in determining whether or not oscillatory behavior occurs. In no case have we found oscillations in a region of parameter space that we consider biologically realistic. The existence of oscillations in a model of this type is not novel. Anderson and May [4] also find oscillatory or chaotic fluctuations in a dynamical model of the interaction of HIV with the immune system. However, they do not discuss the biological implications of the parameters needed to obtain oscillations nor do they map out the regime in parameter space where oscillations ensue.

7. VIRAL INFECTION OF T-CELL PRECURSORS

HIV may be able to infect cells in the thymus and bone marrow and thus lead to a reduced production of new immunocompetent T cells. In

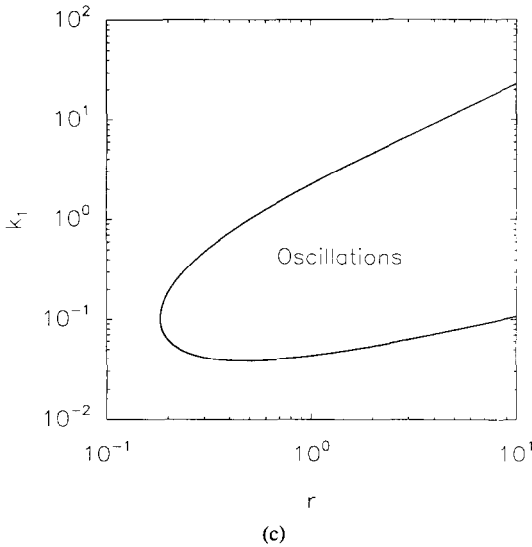


(a)



(b)

FIG. 10. Mapping the region of oscillatory behavior in parameter space. The solid curve indicates the boundary of stability for the infected steady state. As parameters are varied, the state goes unstable and then regains its stability via Hopf bifurcations. In the unstable region, the infected steady state is surrounded by a stable limit cycle. Region of oscillation in the (a) $\mu_T r$ plane; (b) $\mu_T k_1$ plane; (c) $k_1 r$ plane. Parameters not varied are given in Table 2, except $N = 1229.34$.



(c)
FIG. 10 (Continued)

the mouse, CD4 has been shown to be expressed on the earliest thymic T-precursor cells [64]. Whether this is the case in humans has only been speculated about. We examine the consequences of precursor T-cell infection by assuming that the source, s , in Equation (5a) is a decreasing function of the viral load. Perelson [49] assumed $s(v) = se^{-\theta v}$, where θ is a constant. Here, to avoid solving transcendental equations to find the steady state, we shall assume that

$$s(v) = \theta s / (\theta + v). \tag{29}$$

If $v = 0$, then s is a constant as in Equation (1). However, if the viral load increases to the point that $v = \theta$, then s is decreased to half its normal value.

Replacing s by $s(v)$, Equations (5) still have two steady states—an uninfected state and an endemically infected state. In the endemically infected state, \bar{T} , \bar{T}^* , and \bar{T}^{**} are still given by Equations (13a)–(13c). However, \bar{V} is now given by the one positive solution of

$$V^2 [k_1 \mu_V (\alpha + \beta \mu_V)] + V [\theta k_1 \mu_V (\alpha + \beta \mu_V) - p \alpha \mu_V + \gamma \mu_V^2] - \theta [s \alpha^2 + p \alpha \mu_V - \gamma \mu_V^2] = 0. \tag{30}$$

To see that there is only one positive solution, note that in the limit of

large θ we can ignore the terms not proportional to θ in Equation (30). Thus,

$$\bar{V} = \frac{s\alpha^2 + p\alpha\mu_V - \gamma\mu_V^2}{k_1\mu_V(\alpha + \beta\mu_V)}. \quad (31)$$

This is the result that we obtained previously, when s was constant [see Eq. (13d)]. Further, as we showed previously, if $N > N_{\text{crit}}$, then \bar{V} in (31) is positive. Thus, for $N > N_{\text{crit}}$, the last term in (30) is negative. The first term is positive. Thus, regardless of whether the middle term is positive or negative, Equation (30) always has one sign change. Consequently, by Descartes' rule of signs, there will be only one positive root. Thus the effect of replacing s by $s(v)$ will be quantitative, not qualitative. However, as we show below, our model with infection of T-cell precursors gives more realistic predictions for the time course of T-cell depletion.

Figure 11 shows a numerical solution of Equations (5) with s replaced by $s(v)$, using the standard parameters (Table 1) with $\theta = 1 \text{ mm}^{-3}$. The depletion of uninfected cells is now more gradual than in Figures 2, 3, and 5–7. With $N = 1000$, depletion takes about 4 years. Further, the fraction of latently infected cells now remains on the order of 1% or less, as is seen in AIDS patients [51, 55], and the fraction of actively infected cells is less than 2×10^{-4} , consistent with the observations of Harper et al. [24]. Thus this version of the model makes predictions that are consistent with a number of quantitative observations. The one feature that it does not match is the ultimate degree of T-cell depletion, which in AIDS patients commonly decreases below 200 mm^{-3} . Further modifications of the model that might correct this deficiency are presented in Section 10.

8. EFFECTS OF AZT

One of the most successful treatments for AIDS involves the administration of drugs, such as azidothymidine (AZT), that can block viral replication. The effects of such a drug can easily be understood within the context of our model.

The effects of AZT are both dosage-dependent and HIV strain-dependent [35]. Assume that at some time τ AZT is administered and causes a block of viral replication. If viral replication is completely blocked, then for times $t > \tau$, $N = 0$. However, because AZT becomes cytotoxic at high doses, partial blockage is the more likely outcome of AZT treatment. Thus, we assume that for times $t > \tau$, $N = N'$, where $N' < N$. If, before drug administration, $N < N_{\text{crit}}$, then the virus would

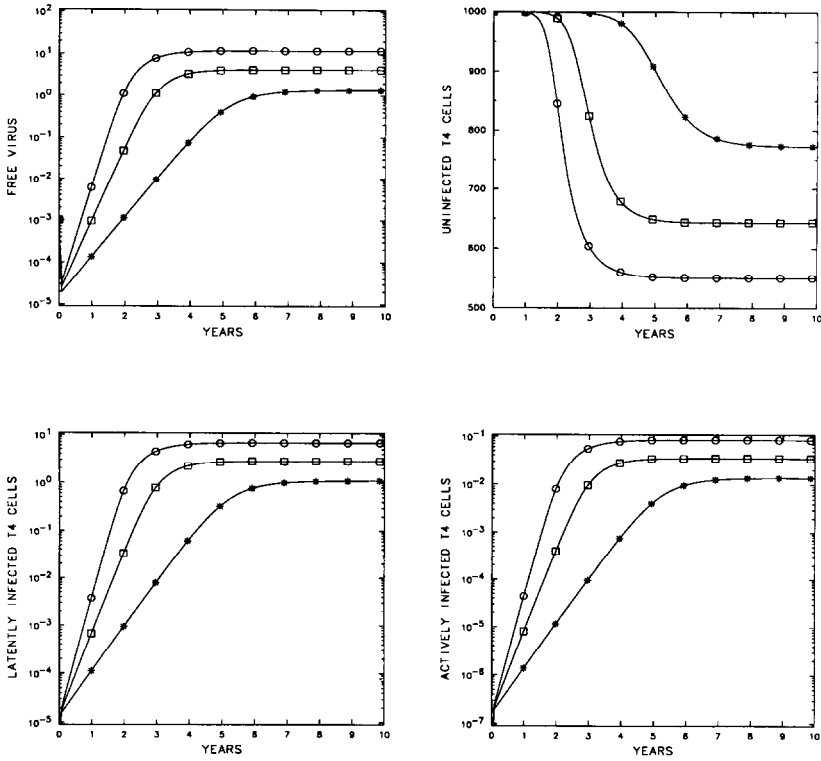


FIG. 11. Viral infection of T-cell precursors. The same model as in Figure 4 is illustrated, except here the source term s decreases with the viral load according to Equation (29) with $\theta = 1 \text{ mm}^{-3}$. Parameters are as in Table 1; $N_{\text{crit}} = 774$ and $N = 1000$ (*), 1200 (\square), 1400 (\circ).

be declining ($dV/dt < 0$) and the drug would simply hasten its elimination. In such cases the drug may not be needed. However, if $N > N_{\text{crit}}$ before treatment, the virus would have been growing, as would the populations of infected T cells. After drug treatment, if $N' < N_{\text{crit}}$, then V , T^* , and T^{**} would all decline and, assuming that the virus had not affected the thymus or T-cell precursors, T would eventually recover to its initial value T_0 . This is illustrated in the upper right panel of Figure 12 (curves marked with circles). If AZT is given in low doses, then even after treatment N may be larger than N_{crit} , so that only partial recovery of the T-cell population occurs (curves with open squares in Figure 12). Partial recovery may also occur if thymic or bone marrow infection occurred or if AZT affected the stem cells responsible for the generation of new T cells. Under such circumstances the source of new cells, s ,

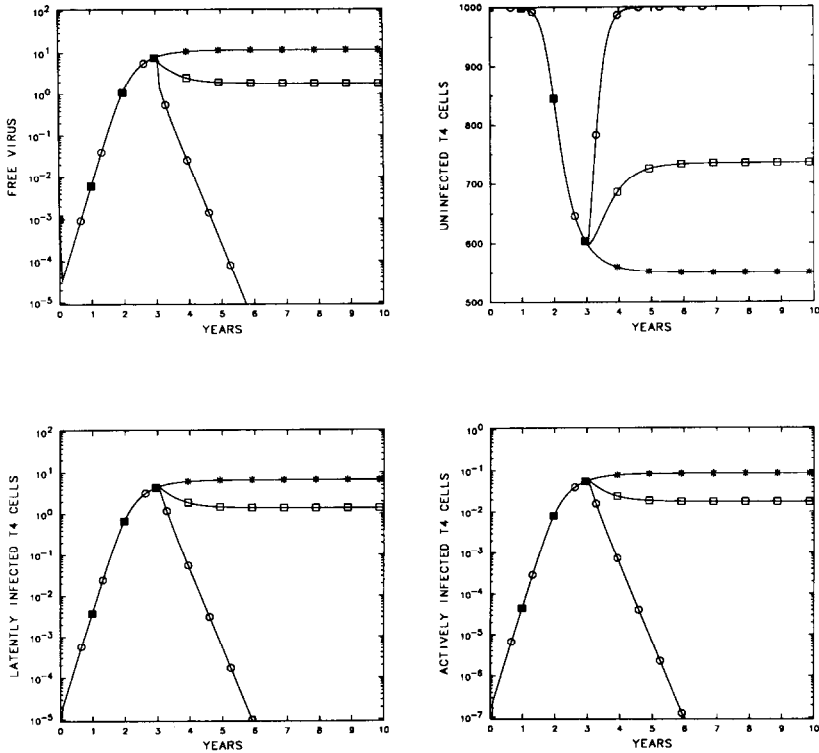


FIG. 12. Effects of AZT. At time $\tau = 3$ years, N is reduced from $N = 1400$ (*) to $N = 1050$ (\square), that is, 75% of its original value, or to $N = 350$ (\circ), that is, 25% of its original value, to mimic the effects of AZT treatment. Here $N_{crit} = 774$, so $N = 1050$ is above N_{crit} , while $N = 350$ is well below N_{crit} . Parameters are as in Table 1.

could be diminished, so that even after treatment and viral elimination the T-cell population would establish a new steady state consistent with a decreased value of s , as is typically the case after adult thymectomy.

9. QUASI-STEADY-STATE APPROXIMATION TO THE DYNAMICS

The total dynamical picture seems to naturally break up into three distinct time domains. In the first, virus rapidly binds to T cells. This corresponds to the rapid initial decay in the free virus population seen in Figure 4. Next, virus and infected T cells increase exponentially, and uninfected T cells maintain a population level close to T_0 . In the last region, uninfected T cells decline in number, the virus and infected T-cell population growth slows, and steady state is established. In this

section we approximate the dynamics in these regions and estimate the time intervals for each type of behavior. We also show how one can use a quasi-steady-state approximation to obtain either a one- or two-dimensional reduced description of the long-time behavior of the system.

9.1. EARLY TIME BEHAVIOR

Assume that the initial conditions are $V(0) = V_0$, $T(0) = T_0$, $T^*(0) = 0$, and $T^{**}(0) = 0$, that is, that infection is by free virus. The earliest event is the binding of virus to uninfected T cells. As can be seen in Figure 4, this causes a rapid decrease in the concentration of free virus. We estimate the depletion of free virus as follows.

Initially, and at early times, $T(t) \simeq T_0$ and $T^{**}(t) \simeq 0$. We use a method of successive approximation to refine these estimates. Thus, first assume that $T = T_0 = \text{constant}$, and $T^{**}(t) = 0$. Equation (5d) then becomes

$$\frac{dV}{dt} = -k_4V,$$

where

$$k_4 = k_1T_0 + \mu_V. \quad (32)$$

Hence virus decays exponentially according to

$$V(t) = V_0e^{-k_4t}. \quad (33a)$$

During this initial period some infection of T cells occurs. From Equation (5a), with $T = T_0$,

$$\begin{aligned} \frac{dT}{dt} &= s - \mu_T T_0 + rT_0(1 - T_0) - k_1T_0V_0e^{-k_4t} \\ &= -k_1T_0V_0e^{-k_4t}, \end{aligned}$$

with solution

$$T(t) = T_0 \left[1 - \frac{k_1V_0}{k_4}(1 - e^{-k_4t}) \right]. \quad (33b)$$

If $k_1V_0 \ll k_4$, $T(t) \simeq T_0$. For the parameters used to generate Figure 4, $k_1V_0/k_4 \simeq 10^{-6}$, and hence there is no observable depletion of T cells.

From Equation (5b),

$$\frac{dT^*}{dt} = k_1T_0V_0e^{-k_4t} - k_3T^*,$$

and thus

$$T^*(t) = \frac{k_1 T_0 V_0}{k_4 - k_3} (e^{-k_3 t} - e^{-k_4 t}). \quad (33c)$$

From (5c) these latently infected cells can create actively infected cells. Substituting (33c) into (5c) and solving yields

$$T^{**}(t) = \frac{k_2 k_1 T_0 V_0}{k_4 - k_3} \left(\frac{e^{-k_4 t}}{k_4 - \mu_b} + \frac{e^{-k_3 t}}{\mu_b - k_3} + \frac{(k_4 - k_3)e^{-\mu_b t}}{(k_4 - \mu_b)(\mu_b - k_3)} \right). \quad (33d)$$

Substituting (33a) into (5d) for $V(t)$, we find

$$\frac{dV}{dt} = N\mu_b T^{**} - k_4 V_0 e^{-k_4 t}, \quad (34)$$

where $T^{**}(t)$ is given by (33d). Although this equation can be used to generate the next-order approximation to $V(t)$, we shall use it to estimate the time at which V stops decreasing, that is, when $dV/dt = 0$. From Equation (34), this occurs at $t = t_{\min}$, where t_{\min} is the solution of the transcendental equation

$$\frac{n\mu_b k_2 k_1 T_0}{\mu_b - k_3} \left(\frac{e^{-k_3 t}}{k_4 - k_3} - \frac{e^{-\mu_b t}}{k_4 - \mu_b} \right) - \left(k_4 - \frac{N\mu_b k_2 k_1 T_0}{(k_4 - k_3)(k_4 - \mu_b)} \right) e^{-k_4 t} = 0. \quad (35)$$

Further, at t_{\min} ,

$$V = V_{\min} = V_0 e^{-k_4 t_{\min}}. \quad (36)$$

Evaluating t_{\min} and V_{\min} for the parameters used to generate Figure 4, we find that with $N = 1000$, $t_{\min} = 2.3$ days and $V_{\min} = 4.2 \times 10^{-6}$. Solving the full system (5) numerically for the same parameters gives $t_{\min} = 2$ days and $V_{\min} = 3 \times 10^{-5}$. These approximations are sufficiently accurate for our purposes and show that the initial decrease in V due to the binding and infection of T cells is quite rapid.

9.2. MIDTERM AND LONGTERM BEHAVIOR

In Figure 2, one immediately obvious feature is that the $T^{**}(t)$, $T^*(t)$, and $V(t)$ curves all look similar. This motivates us to use a

quasi-steady-state analysis to simplify the system. Due to rapid absorption by $CD4^+$ cells, we expect that after a fast transient, the level of free virus will be well approximated by its quasi-steady-state level. Similarly, actively infected cells equilibrate rapidly with latently infected cells. Assuming that on a long time scale $dT^{**}/dt = dV/dt = 0$ leads to the algebraic equations

$$T^{**} = k_2 T^* / \mu_b \quad (37)$$

and

$$V = Nk_2 T^* / (k_1 T + \mu_v). \quad (38)$$

Substituting into Equations (5a) and (5b) leads to

$$\frac{dT}{dt} = s + pT - \gamma T^2 - \left(k_3 \beta + \frac{Nk_1 k_2}{k_1 T + \mu_v} \right) T T^*, \quad (39a)$$

$$\frac{dT^*}{dt} = \frac{Nk_1 k_2}{k_1 T + \mu_v} T T^* - k_3 T^*. \quad (39b)$$

The solution of this two-differential-equation model is shown in Figure 13. As initial conditions we used $T(0) = T_0$ and computed $T^*(0)$ from Equation (33c) evaluated at $t = t_{\min}$. Comparing with Figures 2 and 3, one notices that the solutions are very similar to the solutions of the full system of equations, (5a)–(5d), although there is a detectable difference in the time needed to reach steady state.

The two-equation model can be studied by the usual methods of phase-plane analysis. Figure 14 shows the nullclines of Equations (39a) and (39b) for $N = 600$ and $N = 1400$. When $dT^*/dt = 0$, $T^* = 0$ or $T = \text{constant} = k_3 \mu_v / (Nk_1 k_2 - k_3 k_1)$. These nullclines are indicated by the straight heavy lines in Figure 14. The lighter curved line is the locus of points along which $dT/dt = 0$. Notice that for $N < N_{\text{crit}}$, Figure 14a the two nullclines only intersect at $T = 1000$, $T^* = 0$, the uninfected state. When $N > N_{\text{crit}}$, in addition to this uninfected state, there is a second intersection that corresponds to the endemically infected state. Thus, this phase plane summarizes the general features of the full four-equation model.

During the initial and middle phases of the infection, a good approximation to T is T_0 . Thus, during this period we can substitute $T = T_0$ into (39b) and obtain

$$\frac{dT^*}{dt} = \eta T^*, \quad (40)$$

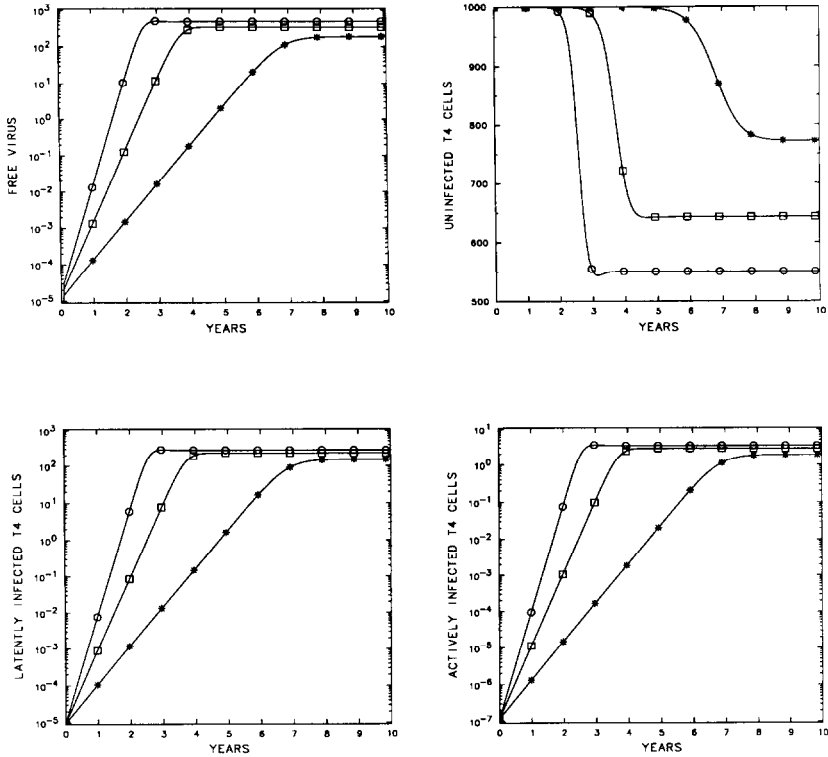


FIG. 13. The quasi-steady-state approximation. Illustrated is the solution of Equations (39) for T and T^* , with $T(0) = 1000$ and $T^*(0)$ given by (33c) with $t = t_{\min}$. The algebraic equations (37) and (38) were used to determine T^{**} and V . Parameters are as in Table 1; $N = 1000$ (*), 1200 (\square), 1400 (\circ).

where

$$\eta = \frac{Nk_1k_2T_0}{k_1T_0 + \mu_V} - k_3 = \frac{k_3(N - N_{\text{crit}})}{N_{\text{crit}}}. \quad (41)$$

From this we predict

$$T^*(t) = T_0^*e^{\eta t}, \quad (42)$$

where T_0^* is determined by matching with a fast-time solution. The time scale $1/\eta$ depends on the difference between N and N_{crit} . Thus, as seen in the simulations, the infection is slow when N is near N_{crit} and becomes fast as N increases. Substituting (42) into (38) with $T = T_0$

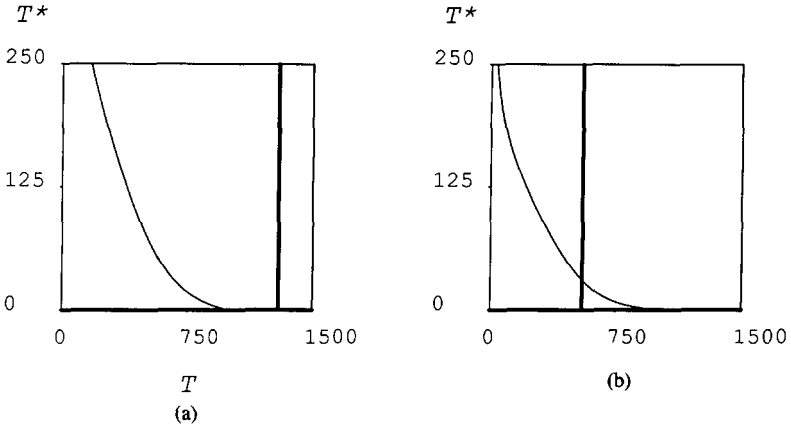


FIG. 14. Nullclines of the reduced two-equation model (39a) and (39b) for (a) $N = 600$ and (b) $N = 1400$. Other parameters are as in Table 1. The light curved line is the $dT/dt = 0$ nullcline, while the two heavy straight lines are the $dT^*/dt = 0$ nullclines. Note that for $N < N_{\text{crit}}$, (a), the nullclines intersect only at the uninfected state $T = 1000$, $T^* = 0$, while for $N > N_{\text{crit}}$, (b), there is a second intersection corresponding to the endemically infected state.

yields

$$V(t) = V_0^+ e^{\eta t}, \quad (43)$$

where $V_0^+ = Nk_2T_0^*/k_4$. Rather than using a formal matching procedure to find T_0^* , we can simply take V_{min} as an approximation to V_0^+ .

10. DISCUSSION

Starting from a description of T-cell population dynamics in a healthy individual, we have developed a dynamical model for T-cell depletion due to HIV infection. While our model is overly simple in that it does not account for the immune response to HIV infection or mechanisms of cell death other than direct HIV-mediated killing, it does demonstrate that HIV by itself can cause partial CD4^+ T-cell depletion in the face of normal T-cell replenishment. Further, the model demonstrates that the loss of T cells can take place on a time scale of years, as is characteristic of the disease process in most HIV-infected individuals.

We considered two forms of the model. In the first, s , the rate of T-cell production from precursors, is constant. In this case we find that T-cell depletion begins between 3 and 6 years after infection and occurs over a period of 1–3 years depending on the value of N , the number of

new virions produced by an infected CD4⁺ T cell (Figures 2 and 3). However, the number of latently infected cells grows to unrealistically high levels, where over 10% of the T cells are infected. Partially because the number of latently infected cells is so large, the depletion of total CD4⁺ T cells is not as dramatic as is seen in patients. The total number of T cells decreases from 1000 mm⁻³ to 830 mm⁻³ when $N = 1400$ (Figure 3). Modifying the model so that s decreases with increasing viral burden, mimicking the effects of infection of T-cell precursors, we obtain dynamics more reminiscent of clinical data. The onset of T-cell depletion is again delayed a few years from initial infection, but the depletion is now more gradual, taking between 3 and 5 years depending on the value of N (Figure 11). Further, the depletion drives the T-cell count substantially lower, with N diminishing from 1400 to approximately 550 mm⁻³ (Figure 11). More important, this depletion is accomplished with between 1 in a 100 and 1 in 1000 T cells latently infected and 1 in 10⁴ cells actively infected, precisely the numbers seen in AIDS patients [55]. Thus, with infection of CD4⁺ T cells as well as precursors, using what we consider to be reasonable parameter values, we obtain realistic kinetics and realistic levels of T-cell infection. However, we find that the T-cell level can be depleted only to a count of approximately 500 mm⁻³, not to the < 200 mm⁻³ level seen in many AIDS patients.

Modifications of the model that include more realistic assumptions about the biology of HIV may correct this deficiency. By increasing N (Figure 5) or k_1 (not shown), more depletion can be obtained, but the rate of depletion becomes unrealistically rapid. This suggests, for example, that if N increases with time, rather than being constant, one may be able to attain more realistic levels of depletion on the correct time scale. Preliminary simulations (not shown) confirm this. A switch from slowly to rapidly replicating strains of virus, which is observed as HIV-infected patients progress from latent to active AIDS, would correspond to an increase in N with time. (Also, a decline in the potential to generate an immune response to HIV as the disease progresses would in some respects correspond to an increase in the effective value of N .) An increase in k_1 with time would correspond to the establishment of a more infectious mutant strain.

One of the interesting predictions of our model is that N , the number of infectious viral particles produced per actively infected T cell, needs to be above some critical level, N_{crit} , for successful HIV infection. If $N < N_{\text{crit}}$, then the level of free virus will monotonically decrease and ultimately be eliminated. This decrease is due to the fact that virus binds and infects cells. If infected cells die without producing a sufficient number of viral progeny, the infection will not be sustained.

In this respect our model is similar to a classical epidemiological model in which infected individuals must infect at least a critical number of other individuals for an epidemic to occur [25]. As in epidemiological models, such as the Lajmanovich and Yorke [32] model for gonorrhea, we find that our model has two steady states, an uninfected steady state in which there is no virus present and no infected T cells, and an endemically infected steady state in which both virus and infected T cells are stably maintained. Because there is depletion in both the number of uninfected T cells and total number of T cells, we expect that immune function would be compromised in the endemically infected state and clinical symptoms of AIDS would appear. This is in agreement with the Walter Reed classification scheme for determining the stage of disease based on the $CD4^+$ T cell cell count in the blood.

Experimental evidence supports our prediction of a critical value for N . Virus isolated from patients has been characterized as being “rapid/high” or “slow/low” [15, 45], where rapid/high indicates that the virus replicates rapidly in culture and shows a high level of reverse transcriptase activity. Slow/low virus exhibit low levels of reverse transcriptase activity and grows slowly. Fenyő et al. [15] find that some slow/low viruses could not be grown in activated peripheral blood mononuclear cells of normal donors. This lack of successful transmission did not seem to be dependent on the amount of virus introduced into the culture, as increasing the amount of infectious virus in the initial inoculum 50-fold had no effect. This lack of successful growth and the phenomenon’s independence from the initial viral population size, V_0 , is precisely what our model predicts for viral strains with $N < N_{crit}$. Further, as one would predict from our model, there is a correlation between the replication potential of a virus and the clinical condition of the patient from whom the virus originated. Thus, viruses isolated from patients with severe immunodeficiency tend to be rapid/high, whereas virus isolated from HIV-infected individuals with no or mild clinical symptoms tend to be slow/low [5, 6, 15]. In general agreement with these results, Tersmette et al. [59] found a significant correlation between the mean replication rate of viral isolates obtained from an individual and the rate of $CD4^+$ cell decrease observed in this individual. In individuals with low-replicating strains, no significant $CD4^+$ cell loss was observed, whereas recovery of high-replicating isolates was associated with rapid decline in $CD4^+$ cell numbers and development of ARC or AIDS. Our current model considers only a single virus population. Clearly, to do a better job of modeling the differences between slow/low and rapid/high strains and the possible transitions between phenotype by mutation requires a model with

multiple HIV populations. Recent work by Nowak et al. [48] and Nowak and May [47] points in this direction.

From the model presented in this paper we conclude that HIV cytopathicity is a major factor in producing many of the quantitative features of HIV infection. Our model shows that HIV cytopathicity of both peripheral CD4⁺ T cells and their precursors gives rise to T-cell depletion, that it can account for the long latency from infection to symptomatic disease, and that it can account for the low levels of infected T cells seen in seropositive patients. However, infection and direct T-cell killing by a *single* viral strain, as depicted in our model, is probably not the only factor involved in T-cell depletion. Changes in cytopathicity (i.e., increases in N or k_1 or a decrease in μ_V) due to the rapid mutation of HIV probably also contribute to the observed phenomenology. Further, the killing of uninfected T cells by other mechanisms, such as syncytium formation or autoimmune reactions, is not ruled out by our model. However, our results show that such mechanisms need not play a major role to get the observed quantitative phenomenology.

We thank George Nelson, Stephen J. Merrill, and James M. Hyman for critical comments and suggestions. We also thank George Nelson for technical assistance. This work was performed under the auspices of the U.S. Department of Energy and supported by the Center for Nonlinear Studies, Los Alamos National Laboratory, and the Santa Fe Institute through their Theoretical Immunology Program, as well as by grants from the University of California Universitywide Task Force on AIDS (R89LANL003) and the National Institutes of Health (AI28433 and RR06555).

REFERENCES

- 1 T. Abo, T. Kawate, K. Itoh, and K. Kumagai, Studies on the bioperiodicity of the immune response. I. Circadian rhythms of human T, B, and K cell traffic in the peripheral blood, *J. Immunol.* 126:1360–1363 (1981).
- 2 J. Albert, B. Abrahamsson, K. Nagy, E. Aurelius, H. Gaines, G. Nyström, and E. M. Fenyö, Rapid development of isolate-specific neutralizing antibodies and consequent emergence of virus variants which resist neutralization by autologous sera, *AIDS* 4:107–112 (1990).
- 3 R. M. Anderson, Mathematical and statistical studies of the epidemiology of HIV, *AIDS* 3:333–346 (1989).
- 4 R. M. Anderson and R. M. May, Complex dynamical behavior in the interaction between HIV and the immune system, in *Cell to Cell Signalling: From Experiments to Theoretical Models*, A. Goldbeter, Ed., Academic, New York, 1989, pp. 335–349.

- 5 B. Åsjö, L. Morfeldt-Månson, J. Albert, G. Biberfeld, A. Karlsson, K. Lidman, and E. M. Fenyö, Replicative capacity of human immunodeficiency virus from patients with varying severity of infection, *Lancet* ii: 660–662 (1986).
- 6 C. Cheng-Mayer, D. Seto, M. Tateno, and J. A. Levy, Biologic features of HIV-1 that correlate with virulence in the host, *Science* 240:80–82 (1988).
- 7 L. N. Cooper, Theory of an immune system retrovirus, *Proc. Natl. Acad. Sci. U.S.A.* 83:9159–9163 (1986).
- 8 R. J. De Boer, *GRIND: Great Integrator of Differential Equations*, Bioinformatics Group, Univ. Utrecht, The Netherlands, 1983.
- 9 E. J. Doedel, AUTO: a program for the bifurcation analysis of autonomous systems, *Cong. Num.* 30:265–285 (1981).
- 10 J. Doležal and T. Hraba, Application of the mathematical model of immunological tolerance to HIV infection, *Folio Biol. (Praha)* 34:336–341 (1988).
- 11 A. S. Edelman, and S. Zolla-Pazner, AIDS: a syndrome of immune dysregulation, dysfunction, and deficiency, *FASEB J.* 3:22–30 (1989).
- 12 H. N. Eisen, *Immunology*, 2nd ed., Harper and Row, Hagerstown, Md., 1980.
- 13 A. S. Fauci, Current issues in developing a strategy for dealing with the acquired immunodeficiency syndrome, *Proc. Natl. Acad. Sci. U.S.A.* 83:9278–9283 (1986).
- 14 A. S. Fauci, The human immunodeficiency virus: infectivity and mechanisms of pathogenesis, *Science* 239:617–622 (1988).
- 15 E. M. Fenyö, L. Morfeldt-Månson, F. Chiodi, B. Lind, A. v Grerfelt, J. Albert, E. Olausson, and B. Åsjö, Distinct replicative and cytopathic characteristics of human immunodeficiency virus isolates, *J. Virol.* 62:4414–4419 (1988).
- 16 J. E. Fletcher, R. I. Shrager, and J. J. Bailey, A kinetic model of T-lymphocyte interactions with HIV, Preprint, 1988.
- 17 T. Folks, J. Kelly, S. Benn, A. Kinter, J. Justement, J. Gold, R. Redfield, K. W. Sell, and A. S. Fauci, Susceptibility of normal human lymphocytes to infection with HTLV-III/LAV, *J. Immunol.* 136:4049–4053 (1986).
- 18 A. A. Freitas, B. Rocha, and A. A. Coutinho, Lymphocyte population kinetics in the mouse, *Immunol. Rev.* 91:5–37 (1986).
- 19 H. R. Gelderblom, E. H. S. Hausmann, M. Özel, G. Pauli, and M. A. Koch, Fine structure of human immunodeficiency virus (HIV) and immunolocalization of structural proteins, *Virology* 156:171–176 (1987).
- 20 J. J. Goedert, R. J. Biggar, M. Melbye, D. L. Mann, S. Wilson, M. H. Gail, R. J. Grossman, R. A. DiGioia, W. C. Sanchez, S. H. Weiss, and W. A. Blattner, Effect of T4 count and cofactors on the incidence of AIDS in homosexual men infected with human immunodeficiency virus, *JAMA* 257:331–334 (1987).
- 21 S. D. Gowda, B. S. Stein, N. Mohaghehpour, C. J. Benike, and E. G. Engleman, Evidence that T cell activation is required for HIV-1 entry in CD4⁺ lymphocytes, *J. Immunol.* 142:773–780 (1989).
- 22 D. Gray, T cell and B cell memory are short lived in the absence of antigen, *J. Cell. Biochem. Suppl.* 13A: C010 (1989).
- 23 D. Gray and T. Leanderson, Expansion, selection and maintenance of memory B cell clones, *Curr. Topics Microbiol. Immunol.* 159:1–17 (1990).
- 24 M. E. Harper, L. M. Marselle, R. C. Gallo, and F. Wong-Stall, Detection of lymphocytes expressing human T-lymphotropic virus type III in lymph nodes and peripheral blood from infected individuals by in situ hybridization, *Proc. Natl. Acad. Sci. U.S.A.* 83:772–776 (1986).

- 25 H. W. Hethcote and J. A. Yorke, *Gonorrhea Transmission Dynamics and Control* (Lect. Notes Biomath. Vol. 56), Springer-Verlag, New York, 1984.
- 26 D. D. Ho, R. J. Pomerantz, and J. C. Kaplan, Pathogenesis of infection with human immunodeficiency virus, *N. Engl. J. Med.* 317:278 (1987).
- 27 J. A. Hoxie, J. D. Alpers, J. L. Rackowski, K. Huebner, B. S. Haggarty, A. J. Cedarbaum, and J. C. Reed, Alterations in T4 (CD4) protein and mRNA synthesis in cells infected with HIV, *Science* 234:1123–1127 (1986).
- 28 T. Hraba and J. Doležal, Mathematical model of CD4⁺ lymphocyte depletion in HIV infection, *Folio Biol. (Praha)* 35:156–163 (1989).
- 29 T. Hraba, J. Doležal, and S. Čelikovsky, Model-based analysis of CD4⁺ lymphocyte dynamics in HIV infected individuals, *Immunobiology* 181:108–118 (1990).
- 30 N. Intrator, G. P. DeCampo, and L. N. Cooper, Analysis of immune system retrovirus equations, in *Theoretical Immunology*, Part 2, A. S. Perelson, Ed., Addison-Wesley, Redwood City, Calif., 1988, pp. 85–100.
- 31 R. Kiernan, J. Marshall, R. Bowers, R. Doherty, and D. McPhee, Kinetics of HIV-1 replication and intracellular accumulation of particles in HTLV-1 transformed cells, *AIDS Res. Hum. Retrovirus* 6:743–752 (1990).
- 32 A. Lajmanovich and J. A. Yorke, A deterministic model for gonorrhoea in a nonhomogeneous population, *Math. Biosci.* 28:221–236 (1976).
- 33 H. C. Lane and A. S. Fauci, Immunologic abnormalities in the acquired immunodeficiency syndrome, *Ann. Rev. Immunol.* 3:477–500 (1985).
- 34 H. C. Lane and A. S. Fauci, Infectious complications of AIDS, in *AIDS: Modern Concepts and Therapeutic Challenges*, S. Broder, Ed., Marcel Dekker, New York, 1987, pp. 185–203.
- 35 B. A. Larder, G. Darby, and D. D. Richman, HIV with reduced sensitivity to zidovudine (AZT) isolated during prolonged therapy, *Science* 243:1731–1734 (1989).
- 36 S. P. Layne, J. L. Spouge, and M. Dembo, Quantifying the infectivity of HIV, *Proc. Natl. Acad. Sci. U.S.A.* 86:4644–4648 (1989).
- 37 R. Leonard, D. Zagury, I. Desportes, J. Bernard, J.-F. Zagury, and R. C. Gallo, Cytopathic effect of human immunodeficiency virus in T4 cells is linked to the last stage of virus infection, *Proc. Natl. Acad. Sci. U.S.A.* 85:3570–3574 (1988).
- 38 A. McLean, HIV infection from an ecological viewpoint, in *Theoretical Immunology*, Part 2, A. S. Perelson, Ed., Addison-Wesley, Redwood City, Calif., 1988, pp. 77–84.
- 39 A. R. McLean and T. B. L. Kirkwood, A model of human immunodeficiency virus infection in T helper cell clones, *J. Theor. Biol.* 147:177–203 (1990).
- 40 J. L. Malone, T. E. Simms, G. C. Gray, K. F. Wagner, J. R. Burge, and D. S. Burke, Sources of variability in repeated T-helper lymphocyte counts from human immunodeficiency virus type 1-infected patients: total lymphocyte count fluctuations and diurnal cycle are important, *J. AIDS* 3:144–151 (1990).
- 41 J. B. Margolick, D. J. Volkman, T. M. Folks, and A. S. Fauci, Amplification of HTLV-III/LAV infection by antigen-induced activation of T cells and direct suppression by virus of lymphocyte blastogenic responses, *J. Immunol.* 138:1719–1723 (1987).
- 42 S. Merrill, AIDS: background and the dynamics of the decline of immunocompetence, in *Theoretical Immunology*, Part 2, A. S. Perelson, Ed., Addison-Wesley, Redwood City, Calif., 1987, pp. 59–75.

- 43 S. Merrill, Modeling the interaction of HIV with cells of the immune response, in *Mathematical and Statistical Approaches to AIDS Epidemiology* (Lect. Notes Biomath., Vol. 83), C. Castillo-Chavez, Ed., Springer-Verlag, New York, 1989, pp. 371–385.
- 44 J. D. Murray, *Mathematical Biology*, Springer-Verlag, New York, 1989.
- 45 P. L. Nara, L. Smit, N. Dunlop, W. Hatch, M. Merges, D. Waters, J. Kelliher, R. C. Gallo, P. J. Fischinger, and J. Goudsmit, Emergence of viruses resistant to neutralization by V3-specific antibodies in experimental human immunodeficiency virus type 1 IIIB infection of chimpanzees, *J. Virol.* 64:3779–3791 (1990).
- 46 G. W. Nelson and A. S. Perelson, A mechanism of immune escape by slow-replicating HIV strains, *J. AIDS* 5:82–93 (1992).
- 47 M. A. Nowak and R. M. May, Mathematical biology of HIV infections: antigenic variation and diversity threshold, *Math. Biosci.* 106:1–21 (1991).
- 48 M. A. Nowak, R. M. May, and R. M. Anderson, The evolutionary dynamics of HIV-1 quasispecies and the development of immunodeficiency disease, *AIDS* 4:1095–1103 (1990).
- 49 A. S. Perelson, Modeling the interaction of the immune system with HIV, in *Mathematical and Statistical Approaches to AIDS Epidemiology* (Lect. Notes Biomath., Vol. 83), C. Castillo-Chavez, Ed., Springer-Verlag, New York, 1989, pp. 350–370.
- 50 A. Phillips, C. A. Lee, J. Elford, G. Janossy, M. Bofill, A. Timms, and P. B. A. Kernoff, Prediction of progression to AIDS by analysis of CD4 lymphocyte counts in a haemophilic cohort, *AIDS* 3:737–741 (1989).
- 51 M. C. Psallidopoulos, S. M. Schnittman, L. M. Thompson, M. Baseler, A. S. Fauci, H. C. Lane, and N. P. Salzman, Integrated proviral human immunodeficiency virus type 1 is present in CD4⁺ peripheral blood lymphocytes in healthy seropositive individuals, *J. Virol.* 63:4626–4631 (1989).
- 52 E. M. Purcell, Life at low Reynolds number, *Am. J. Phys.* 45:3–11 (1977).
- 53 R. R. Redfield, D. C. Wright, and E. C. Tramont, The Walter Reed staging classification for HTLV-III/LAV infection, *N. Engl. J. Med.* 314:131–132 (1986).
- 54 G. Reibnegger, D. Fuchs, A. Hausen, E. R. Werner, M. P. Dierich, and H. Wachter, Theoretical implications of cellular immune reactions against helper lymphocytes infected by an immune system retrovirus, *Proc. Natl. Acad. Sci. U.S.A.* 84:7270–7274 (1987).
- 55 S. M. Schnittman, M. C. Psallidopoulos, H. C. Lane, L. Thompson, M. Baseler, F. Massari, C. H. Fox, N. P. Salzman, and A. S. Fauci, The reservoir for HIV-1 in human peripheral blood is a T cell that maintains expression of CD4, *Science* 245:305–308 (1989).
- 56 S. M. Schnittman, J. J. Greenhouse, M. C. Psallidopoulos, M. Baseler, N. P. Salzman, and A. S. Fauci, Increasing viral burden in CD4⁺ T cells from patients with human immunodeficiency virus (HIV) infection reflects rapidly progressive immunosuppression and clinical disease, *Ann. Int. Med.* 113:438–443 (1990).
- 57 M. Somasundaran and H. L. Robinson, Unexpectedly high levels of HIV-1 RNA and protein synthesis in a cytotoxic infection, *Science* 242:1554–1557 (1988).
- 58 J. M. G. Taylor, J. L. Fahey, R. Detels, and J. V. Giorgi, CD4 percentage, CD4 number and CD4:CD8 ratio in HIV infection: which to choose and how to use, *J. AIDS* 2:114–124 (1989).

- 59 M. Tersmette, R. A. Gruters, F. de Wolf, R. E. Y. de Goede, J. M. A. Lange, P. T. A. Schellekens, J. Goudsmit, H. G. Huisman, and F. Miedema, Evidence for a role of virulent human immunodeficiency virus (HIV) variants in the pathogenesis of acquired immunodeficiency syndrome: studies on sequential HIV isolates, *J. Virol.* 63:2118–2125 (1989).
- 60 G. Tindall and D. A. Cooper, Primary HIV infection, *AIDS* 5:1–14 (1991).
- 61 L. Weiss, *The Cells and Tissues of the Immune System*, Prentice-Hall, Englewood Cliffs, N.J., 1972.
- 62 S. Wiggins, *Introduction to Applied Nonlinear Dynamic Systems and Chaos*, Springer-Verlag, New York, 1990.
- 63 J. L. Willems, *Stability Theory of Dynamical Systems*, Wiley, New York, 1970.
- 64 L. Wu, R. Scollay, M. Egerton, M. Pearse, G. J. Spangrude, and K. Shortman, CD4 expressed on earliest T-lineage precursor cells in adult murine thymus, *Nature* 349:71–74 (1991).
- 65 J. A. Zack, S. J. Arrigo, S. R. Weitsman, A. S. Go, A. Haislip, and I. S. Y. Chen, HIV-1 entry into quiescent primary lymphocytes: molecular analysis reveals a labile, latent viral structure, *Cell* 61:213–222 (1990).